applied sciences

MDPI

Review

Zirconium-Containing Metal–Organic Frameworks (MOFs) as Catalysts for Biomass Conversion

Anastasia Rapeyko * and Francesc X. Llabrés i Xamena *

Instituto de Tecnología Química, Agencia Estatal Consejo Superior de Investigaciones Científicas, Universitat Politècnica de València, Avda. de los Naranjos, s/n, 46022 Valencia, Spain
* Correspondence: arapeyko@itq.upv.es (A.R.); fllabres@itq.upv.es (F.X.L.i.X.)

Abstract: In this work, we review some illustrative examples to evidence the potential of two archetypal Zr-containing MOFs, UiO-66 and MOF-808, as heterogeneous catalysts for converting biomass-derived products into valuable chemicals. The reactions are organized in three blocks, depending on the biomass source: carbohydrates, lipids, and other sources. Through this review, we will show that the chemical properties of these two Zr-MOFs are significantly different in terms of the nature and strength of acid sites, which largely depends on the number of missing linker defects of the solid and its hydration state. While hydrated UiO-66 bears relatively strong Brønsted-induced acid sites, dehydrated MOF-808 is more than competent as a Lewis acid catalyst. Therefore, we will pick one or the other catalyst depending on the particular demands of the catalytic transformation that we want to carry out.

Keywords: biomass into chemicals; Zr-containing metal–organic frameworks; heterogeneous catalysis

1. Introduction

The pressing environmental demands for more sustainable energy sources and renewable raw materials, together with the continuous depletion of oil reserves worldwide, have strongly boosted the interest for developing new routes of biomass valorization, including the preparation of biofuels. The aim of this industrial transformation at a global level is to decrease the dependence on fossil fuels by substituting them with renewable resources and to reduce the emission of greenhouse gases and carbon footprint.

Biomass comprises all the organic matter with a biologic or anthropogenic origin that can be used as feedstock for obtaining energy and chemical products of industrial interest, excluding that of a fossil origin used by the petrochemical industry [1]. According to this definition, this encompasses all the organic matter produced by plants and animals such as trunks, leaves, branches, peels and bones, animal dung, but also wastes or byproducts from the paper, wood, or food industries related with human activities. Other sources of biomass include the so-called energy crops, such as corn, beet, or sugar cane, produced for energy purposes, or marine biomass, including the production of microalgae.

One of the most extended uses of biomass is as an energy source, either by direct transformation into biofuels by gasification to obtain *syn-gas*, or by direct combustion. Nevertheless, there is an increasing interest in recent years in biomass valorization, in which biomass is used as a starting material to produce chemical compounds of industrial interest, known as platform chemicals, which can then be used as intermediates for the synthesis of several bulk and fine chemicals, such as solvents, fuel additives, fragrances,

check for updates

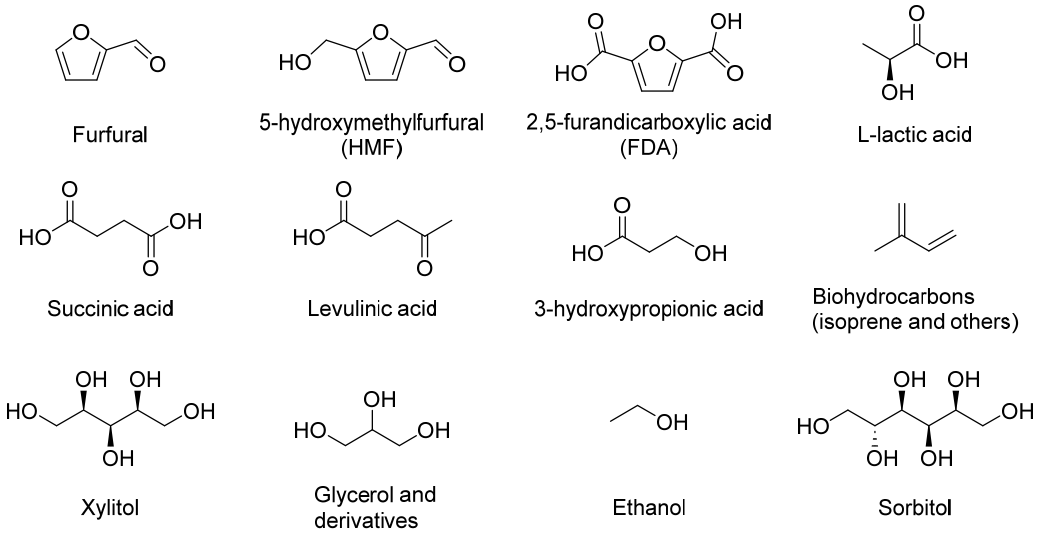
Academic Editor: Luca Fiori

Received: 7 February 2025
Revised: 26 February 2025
Accepted: 26 February 2025
Published: 28 February 2025

Citation: Rapeyko, A.; Llabrés i Xamena, F.X. Zirconium-Containing Metal–Organic Frameworks (MOFs) as Catalysts for Biomass Conversion. *Appl. Sci.* **2025**, *15*, 2609. https://doi.org/10.3390/app15052609

Copyright: © 2025 by the authors. Licensee MDPI, Basel, Switzerland. This article is an open access article distributed under the terms and conditions of the Creative Commons Attribution (CC BY) license (https://creativecommons.org/licenses/by/4.0/).

paints, or biopolymers [2]. Some of the main platform chemicals obtained from biomass include furfural, 5-hydroxymethyl furfural, ethanol, succinic acid, or levulinic acid, among others (see Scheme 1) [3].



Scheme 1. Some of the main platform chemicals obtained from biomass.

The use of heterogeneous catalysis is critical for developing efficient transformation routes for biomass valorization, since it allows easy separation, recovery, and reutilization of the catalyst. Moreover, with the synthetic tools available nowadays, it is possible to design materials with specific catalytic active sites, or even catalysts containing more than one type of sites (multifunctional catalysts) that can be used in cooperative catalysis or in multistep processes. Altogether, this allows us to develop novel transformation routes combining two or more sequential reactions in one single reactor (one-pot cascade reactions), thereby avoiding the isolation and purification of reaction intermediates and reducing the energy consumption of the overall process. In this sense, several solid materials have been considered so far as (multifunctional) heterogeneous catalysts to replace the homogeneous catalysts traditionally used. Those include supported metal catalysts and heteropolyacids, zeolites, metal oxides, and metal–organic frameworks (MOFs).

In the last two decades, we have been intensively involved in our group in using MOFs as heterogeneous catalysts for developing new routes for biomass valorization from various sources. Throughout this review, we will present the most relevant results obtained in this research line by us and other groups. The article is structured depending on the origin of the biomass used, whether carbohydrates, lipids, or other sources. But first, we will briefly describe what are MOFs and why we want to use them as heterogeneous catalysts.

2. Metal–Organic Frameworks (MOFs) and Their Use in Catalysis

MOFs are a subclass of coordination polymers that are characterized by being crystalline, porous solids formed by the linkage of metal ions (or metal oxoclusters) and polydentate organic molecules by metal coordination bonds, forming a crystalline network defining pores of strictly regular dimensions [4,5]. These metal–ligand coordination bonds are stronger and more directional than the hydrogen bonds or π–π stacking interactions typically found in other amorphous, non-porous coordination polymers—hence, the convenience for practical reasons of differentiating the MOFs within the large family of coordination polymers [6]. What has drawn interest in these materials in recent years is that it is possible to fine-tune the framework topology, as well as to control the shape, dimensions, and connectivity of the structural pores, by properly selecting the structural

units (metals and organic ligands) and the way in which they are connected. By a careful selection of the structural units forming the MOF, it has been possible to prepare ultrahigh porous materials that have largely surpassed the specific surface areas and pore volumes found in other porous compounds (such as zeolites, mesoporous silicas, or carbons). Thus, some MOFs feature astonishing specific surface areas over 7000 m^2g^{-1} and pore volumes of 4 cm^3g^{-1} or larger, such as the compounds known as NU-110 (7140 m^2g^{-1} and 4.40 cm^3g^{-1}, respectively) [7] or DUT-60, holding the ultrahigh porosity world-wide record attained so far with 7800 m^2g^{-1} and 5.02 cm^3g^{-1} [8]. When designing a material for heterogeneous catalysis, large specific surface areas and wide pores are a must for ensuring a fast diffusion of reactants and products in and out of the pores to reach the active sites located at the internal surface of the catalyst. Therefore, it is not surprising that since the discovery of MOFs, these compounds have been considered for catalytic applications [9–11]. Moreover, relevant chemical properties, such as Lewis/Brønsted acidity, hydrophilicity/hydrophobicity, the presence of specific functional groups, or the nature and magnitude of noncovalent interactions inside the pores, can be largely determined by the chemical composition of the material. This large tunability of MOFs opens up the possibility to use these materials in size/shape selective reactions. In this way, if we have a mixture of two or more compounds that can be potentially converted in a reaction, only those molecules whose dimensions are small enough to enter the pores of the MOF will reach the catalytic active sites and will be converted, while larger molecules (or with an unappropriated shape) will remain unchanged in the reaction medium. Likewise, if different products or transition states can be competitively formed during a reaction, only those transition states or products that can fit inside the MOF pores will be viable. In other words, by finely tuning the pore size and shape of a MOF, as well as other properties such as the chemical environment inside the cavities, we can drive the reaction towards the formation of the desired product among different possibilities, thereby achieving very high selectivity, emulating the behavior of enzymatic catalysis. Nevertheless, it is always a good practice to compare the results obtained with MOF catalysts with those previously reported in the scientific literature with other catalysts (both homogeneous and heterogeneous), as this allows us to fairly appraise the potential of the MOF for any given reaction.

In the present review on biomass conversion routes over MOFs, we will focus our interest on two families of compounds, namely UiO-66 [12] and MOF-808 [13]. Both of them contain hexanuclear zirconium oxoclusters as the inorganic building block, and carboxylate linkers: terephtalic acid (and derivates) in the case of UiO-66, and trimesic acid (and derivates) in MOF-808. To understand the catalytic properties of these two compounds, and why they behave in a different way as acid catalysts, it is important to know first their structural details, with especial emphasis on their similarities and differences.

3. Structure and Properties of UiO-66 and MOF-808: Origin of Lewis and Brønsted-Induced Acidity

UiO-66 (UiO stands for University of Oslo) is a robust zirconium terephthalate (1,4-benzenedicarboxylate) formed by hexameric $[Zr_6O_4(OH)_4]$ octahedral oxoclusters connected by 12 terephthalate linkers into a face-centered cubic packing. This arrangement of structural units leads to tetrahedral and octahedral cavities of about 8 and 11 Å, respectively; both of them accessible through triangular windows of about 6 Å in diameter (see Figure 1). The high coordination number of the inorganic building units to 12 organic linkers bestows a remarkable thermal, chemical, and mechanical stability [14], which is seldom found in other MOFs. An interesting property of UiO-66 is that Zr^{4+} ions can be replaced by other tetravalent cations (Hf [15], Ce [16], Ti [17], etc.), while terephthalate linkers can be replaced by other linkers with the same geometrical connectivity, including substituted terephtha-

lates, and extended linear carboxylates, such as biphenyl-4,4′-dicarboxylate in UiO-67, *p*-terphenyl-4,4″-dicarboxylate in UiO-68, or the large family of PIZOFs with even longer linkers [18,19]. This affords a battery of isoreticular derivatives available, i.e., materials having the same network topology and pore architecture as UiO-66, but with a tailored pore size and chemical environment inside the cavities, and thus, with tunable properties.

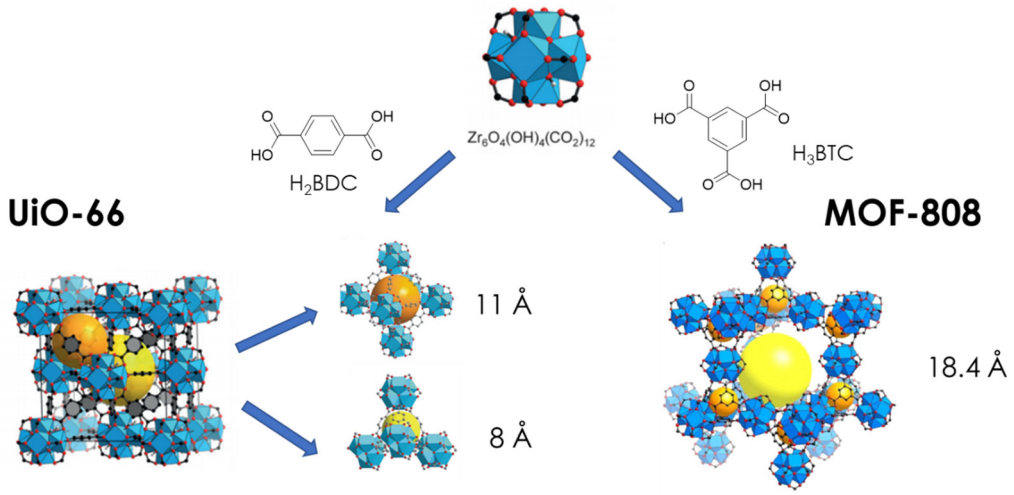
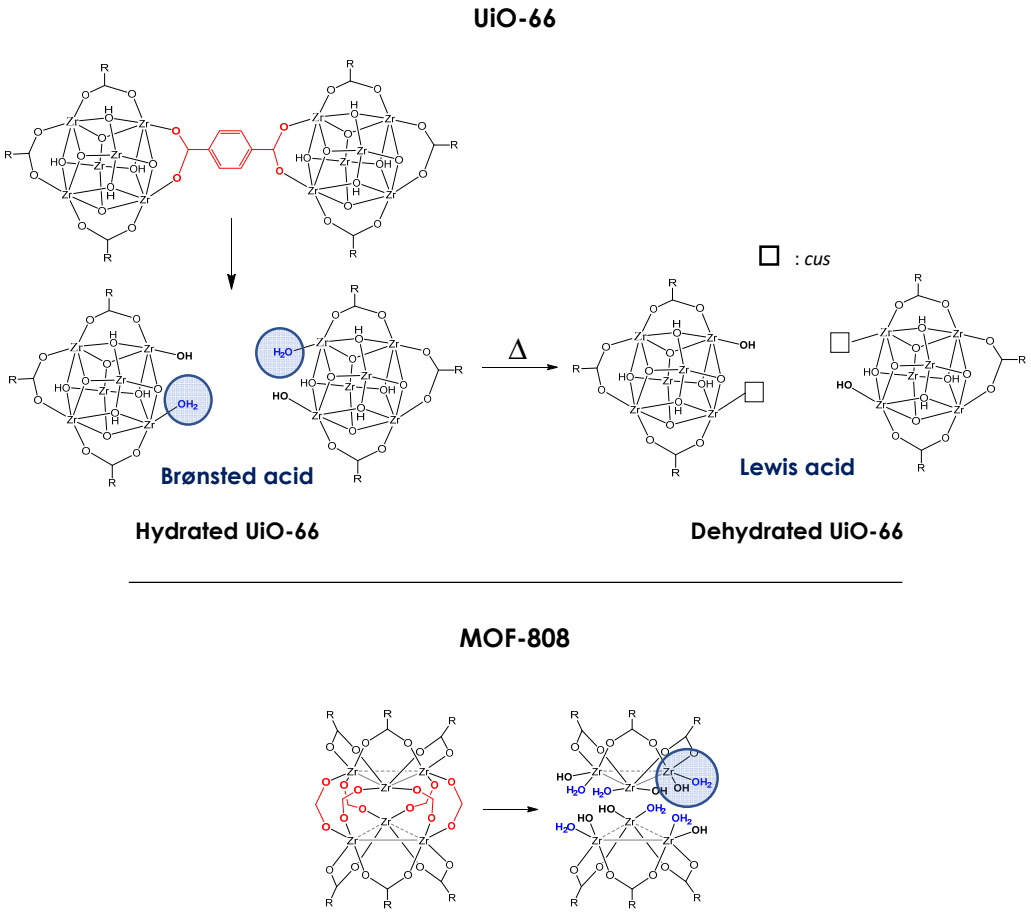


Figure 1. Structure and pore cavities in UiO-66 and MOF-808. Figure adapted from references [12,13]. Copyright 2008 and 2014, American Chemical Society.

In the structure of UiO-66 and related solids, Zr^{4+} ions (or other M^{4+} cations) lack coordination vacancies available for substrate binding, and thus, in the *ideal* UiO-66 structure, Zr^{4+} ions should not behave as Lewis acid sites. However, *real* UiO-66 compounds usually present missing linker defects, either randomly formed during the self-assembly formation of the MOF [20] or intentionally created during or after the synthesis [21]. In this way, the Zr^{4+} ions associated with these missing linker defects feature coordinative unsaturation sites (*cus*), with the ability to accept electron density from species adsorbed inside the pores. In UiO-66, each terephthalate linker is connected to four Zr^{4+} ions. A missing linker defect can be imagined as the removal of one of the twelve negatively charged terephthalate linkers connecting the Zr_6 oxoclusters. When this happens, two of the four Zr ions initially connected by the missing linker are saturated by $^{-}$OH (or Cl^{-}) anions to preserve the electrical neutrality of the material, thus leaving two Zr^{4+} *cus* per missing linker molecule, as shown in Scheme 2. As we have discussed in previous works [22], when the MOF is hydrated, these *cus* will have strongly coordinated water molecules, which will introduce Brønsted-induced acidity in the material. These adsorbed water molecules will be highly polarized due to the high charge-to-radius ratio of Zr^{4+} cations, so the acidity is noticeable. However, these water molecules can be removed by thermal dehydration, exposing the Zr^{4+} sites and making them available as Lewis acid sites. Therefore, it is possible to tune the acid properties of UiO-66-type materials by simply controlling the hydration degree of the material. Throughout this review, we will see examples in which both types of sites can be used effectively to catalyze specific reactions for converting biomass into chemicals. A key aspect to take into account in UiO-66 is that the active sites are associated with defects, so: (i) not all the Zr^{4+} sites will participate in the reaction, and therefore (ii) the catalytic activity will increase with the number of missing linker defects. In other words, we should not expect any catalytic activity for an "ideal", defect-free UiO-66.



Scheme 2. (**Top**) Missing linker defects in hydrated and dehydrated UiO-66. (**Bottom**) Coordination of Zr^{4+} cations in MOF-808 upon removal of formate linkers.

Next to UiO-66, the second protagonist of this review is MOF-808. This is a MOF containing similar Zr_6 oxoclusters connected by trimesate (1,3,5-benzenetricarboxylate) linkers, forming a much wider tridimensional network than UiO-66, with adamantane-shaped cages of 18.4 Å and openings of 14 Å (see Figure 1). A first clear difference between UiO-66 and MOF-808 is that the latter material will be able to adsorb much larger molecules inside the pores, and thus, it will be able to catalyze the transformation of bulkier substrates (see for instance [23]). But this is not the only difference. In MOF-808, each Zr_6 cluster is connected by six trimesate molecules to other clusters (the connectivity in UiO-66 is 12, as commented above), while the rest of the coordination positions of Zr^{4+} are saturated by six bridging formate ions connecting two Zr inside the cluster. These formate linkers can be removed by solvent washing or mild thermal treatment, leaving two coordination vacancies on each Zr^{4+} site. One of them is occupied by an $^{-}$OH group to keep the electrical neutrality of the material, while the second position is either a coordination vacancy (in dehydrated MOF-808) or is occupied by an adsorbed H_2O molecule (in hydrated MOF-808).

Therefore, although both UiO-66 and MOF-808 have similar Zr_6 clusters in their structures, their Brønsted-induced acid properties are completely different, both in number and in acid strength. This is so because the Zr^{4+} *cus* in both materials are also different, as shown in Scheme 2. Note that in MOF-808, all Zr^{4+} sites will participate in the catalytic reaction, unlike in UiO-66, where only a small fraction will be available, depending on the concentration of missing linkers. Also, in MOF-808, each Zr^{4+} is capped by one $^{-}$OH group and one H_2O molecule, simultaneously. Thus, the effective polarizing power of the Zr^{4+} ions over the adsorbed water molecules is largely countered by the geminal $^{-}$OH groups,

so their induced Brønsted acidity is much lower than in UiO-66, in which geminal OH groups are not present.

We can thus summarize the main acid properties of UiO-66 and MOF-808 as follows (Table 1):

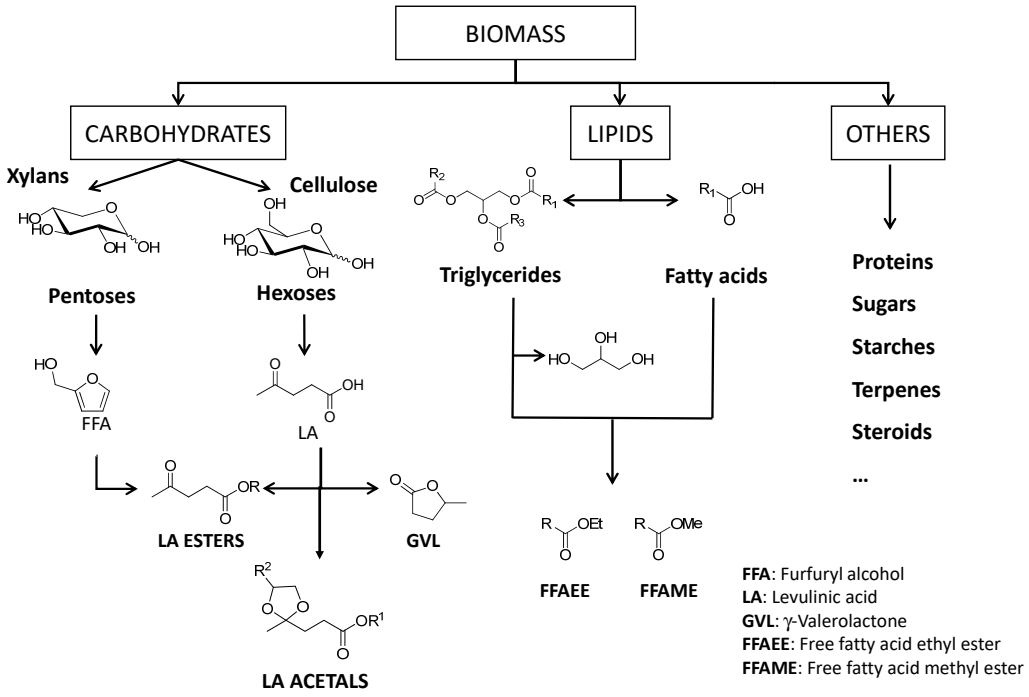
Table 1. Acid properties of hydrated and dehydrated UiO-66 and MOF-808.

	Lewis Acidity (Dehydrated Material)	Brønsted-Induced Acidity (Hydrated Material)
UiO-66	✗ Few acid sites (only at defect sites) ✗ Restricted pore space (hindered Lewis sites)	✓ Strongly polarized H_2O molecules (strong Brønsted sites)
MOF-808	✓ All Zr^{4+} sites available ✓ Wide pores (efficient Lewis sites)	✗ Weakly polarized H_2O molecules due to geminal $^{-}$OH groups (weak Brønsted sites)

4. Conversion of Biomass into Chemicals over UiO-66 and MOF-808

Scheme 3 summarizes some of the main existing routes for converting biomass into chemicals using MOFs as heterogeneous catalysts. Following this very simple (and obviously incomplete) scheme, and to illustrate the great potential of archetypal UiO-66 and MOF-808, in this review we have selected some representative examples from the literature, which have been organized into three blocks, depending on the biomass source, as follows:

- Conversion of carbohydrates;
- Conversion of lipids (fatty acids and glycerol);
- Conversion of other biomass-derived compounds.



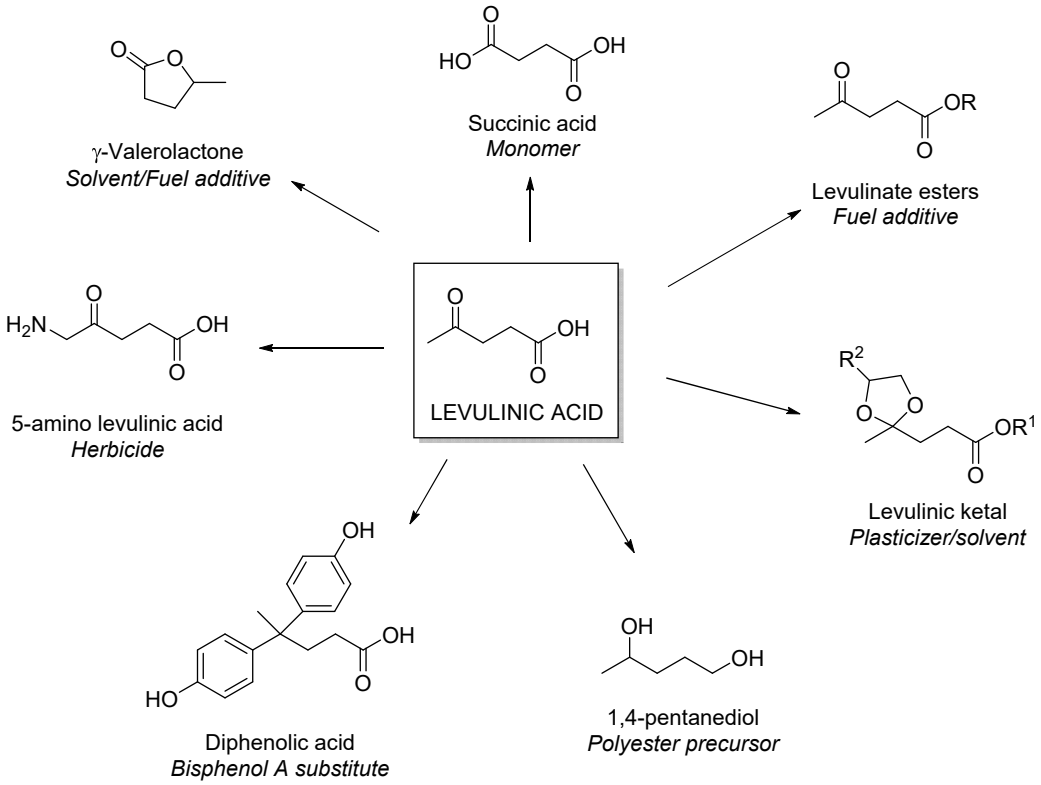
Scheme 3. Main catalytic routes for converting biomass into chemicals.

5. Conversion of Carbohydrates

5.1. Levulinic Acid into Chemicals

5.1.1. Levulinic Acid Derivates as Value-Added Chemicals

Levulinic acid (LA) can be obtained from the deconstruction of several kinds of raw materials, including monosaccharides, polysaccharides, and renewable resources, such as lignocellulosic biomass [2]. LA can be used as a starting material for the synthesis of many other important products in food and chemical industries (Scheme 4), including alkyl levulinate esters, γ-valerolactone, and levulinic ketals [24].



Scheme 4. Main value-added LA derivatives and their uses.

Alkyl levulinate esters have low toxicity, high lubricity, and flashpoint stability (90 °C), as well as moderate flow properties at a low temperature, which make them suitable additives for gasoline and diesel fuels [25]. Ethyl levulinate (EL) can be used as an oxygenated additive in diesel formulations to reduce soot formation by up to 20% of the total content. EL is also suitable in gasolines due to the high octane rating (RON 110, MON 102) and energy content (31.2 MJ/L). The properties of levulinate esters are similar to biodiesel fatty acid methyl esters (FAMEs) but without their drawbacks of low cold flow properties and gum formation. Besides their use as a fuel additive, levulinate esters are also used in other areas, as flavoring compounds and fragrances, solvents, and plasticizers [2]. Levulinic ketals are prepared by reacting LA with polyalcohols in the presence of an acid catalyst. The resulting compounds are used as building blocks for the synthesis of pharmaceuticals, fragrances, plasticizers, cosmetics, or fuel additives [26–30]. Meanwhile, γ-Valerolactone (4,5-Dihydro-5-methyl-2(3*H*)-furanone, GVL) is used as a fuel additive to produce cleaner-burning fuels [24,31], as a biomass-derived solvent [32], as a component of biocide formulations, and as an intermediate for the synthesis of fine chemicals, such as adipic acid, valeric acid [33,34], or 5-nonanone [35].

5.1.2. Synthesis of Levulinate Esters

Given the interest in LA and its derivatives, one of the first reactions studied in our group dealing with biomass conversion over MOF catalysts was the esterification of LA with various alcohols [20]. We reported on the use of UiO-66 and its derivative, UiO-66-NH_2 (containing 2-aminoterephthalate linkers), for the conversion of LA to ethyl levulinate, *n*-butyl levulinate, and various long-chain alkyl levulinates. The relevance of that work, which we will revise now, was that we established, for the first time, that a direct correlation existed between the concentration of missing linker defects and catalytic activity for this type of reaction. Later, we also investigated the reaction mechanism and the influence of amino substituents in the terephthalate ring with ab initio methods [36], and we demonstrated that the active sites for this reaction were Brønsted-induced acid sites formed by strongly polarized water molecules adsorbed onto coordinatively unsaturated Zr^{4+} sites associated with missing linker defects [22].

Thus, our approach consisted of preparing several batches of UiO-66 and UiO-66-NH_2, each of them having a variable amount of missing linker defects comprised between 2.5 and 13.2% for UiO-66, and between 2.1 and 8% for UiO-66–NH_2. The exact amount of missing linker defects in each sample was calculated from the corresponding thermogravimetric curve (TGA), following the method proposed by Valenzano et al. [37]. These linker defects were formed randomly during the synthesis of the MOF, and are most likely due to small differences in nucleation and crystal growth rates during the synthesis from batch to batch. After checking that all catalysts were highly crystalline, we observed that all of them were active for the esterification of LA with ethanol. However, a large variation of the catalytic performance existed from batch to batch. Thus, calculated pseudo-first order kinetic rate constants varied between 0.61 h^{-1} and 0.07 h^{-1} for UiO-66; i.e., an almost 9-fold increase from the less active to the most active catalyst batch. Similar results, although with smaller variations, were found for UiO-66-NH_2, with kinetic rate constants ranging from 0.33 h^{-1} to 0.43 h^{-1}. The time–yield plots obtained for all the catalyst batches are shown in Figure 2.

The linear dependence of the kinetic rate constant on the concentration of the defects of the catalyst is evident from the plot shown in Figure 2c, for both the UiO-66 and UiO-66-NH_2 series of catalysts. Note also that, for a given defect concentration, UiO-66-NH_2 catalysts are, in general, slightly more active that UiO-66. This was first attributed [20] to a cooperative bifunctional acid–base effect of the (Lewis acid) Zr^{4+} sites and the (basic) amino groups of UiO-66-NH_2. Later [36], we used a combination of experimental and ab initio calculations to show that the amino groups in the terephthalate linkers do not participate directly in the esterification reaction. However, their presence in the terephthalate linkers increases the hydrophilic character of the solid and favors water adsorption (more water is adsorbed and the interaction is stronger than in the UiO-66 lacking amino groups). And these adsorbed water molecules do participate directly in the esterification reaction. Meanwhile, catalyst particle size has a different effect on UiO-66 (catalytic activity independent of particle size) and UiO-66-NH_2 (lower activity as the particle size increases), as shown in Figure 2d. This indicates that there is no diffusion control of the esterification reaction in UiO-66. On the contrary, the amino groups reduce the free pore openings of UiO-66-NH_2, due to the large size of -NH_2 groups (of aminoterephthalate linkers) with respect to -H (in terephthalate linkers). This prevents or at least hinders the diffusion of LA into the MOF pores of UiO-66-NH_2. In this way, the reaction should take place mainly at the external surface of the catalyst.

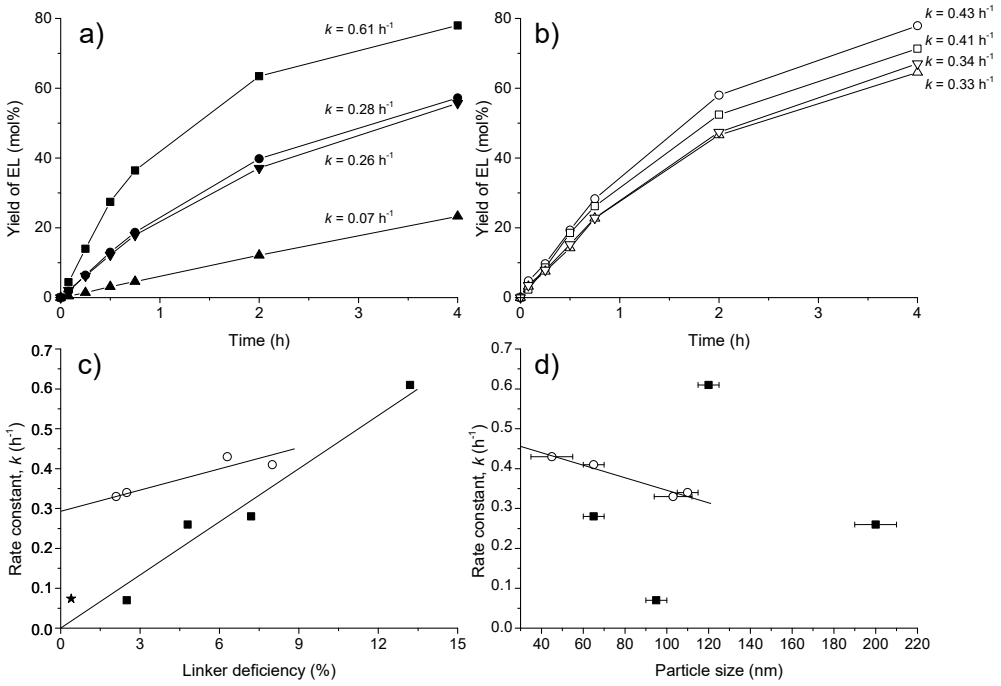


Figure 2. Yield of ethyl levulinate (EL) obtained over four different batches of (**a**) UiO-66 and (**b**) UiO-66-NH_2. For each curve, the calculated pseudo-first order kinetic rate constant is indicated (**c**); dependency of the esterification pseudo-first order rate constant (*k*) on the linker deficiency of the catalyst. Closed and open symbols for UiO-66 and UiO-66-NH_2, respectively; (**d**) dependency of the esterification rate constant on the particle size of the catalyst. Error bars represent the size dispersion (95% confidence interval) for each catalyst. Same symbols as in part (**c**) for UiO-66 and UiO-66-NH_2. Reproduced with permission from reference [20]. Copyright (2015) Elsevier.

Given the excellent results obtained for the synthesis of ethyl levulinate, we wanted to test the performance of UiO-66 catalysts for the synthesis of other interesting levulinate esters [20]. Thus, we prepared *n*-butyl levulinate and esters with biomass-derived long chain monohydric aliphatic alcohols with equally good results.

It is interesting to determine the exact nature of the active sites in UiO-66 that catalyze the esterification reaction, as well as the influence of the hydration degree of the catalyst. To do so, we compared the catalytic activity of hydrated and dehydrated UiO-66 [22], and we observed a definite decrease in the catalytic activity upon dehydration. We also found that a clear interdependence exists between some key parameters of UiO-66; namely, the amount of linker defects, the amount and strength of adsorbed water molecules, the hydration degree of the solid, and the Brønsted acidity of the solid, in terms of the pH measured from a methanolic dispersion of UiO-66. All these parameters are tightly correlated and they all determine the final catalytic activity for esterification [22]. This is evidenced in Figure 3, where we plotted the logarithm of the kinetic rate constant for LA esterification, log *k*, versus the measured pH after dispersing various MOFs and other heterogeneous or homogeneous catalysts in methanol. This strong correlation between k and the pH decrease in methanol produced by the catalyst clearly suggests that the Brønsted-induced acid sites of the MOF are the most likely active sites for the esterification of LA.

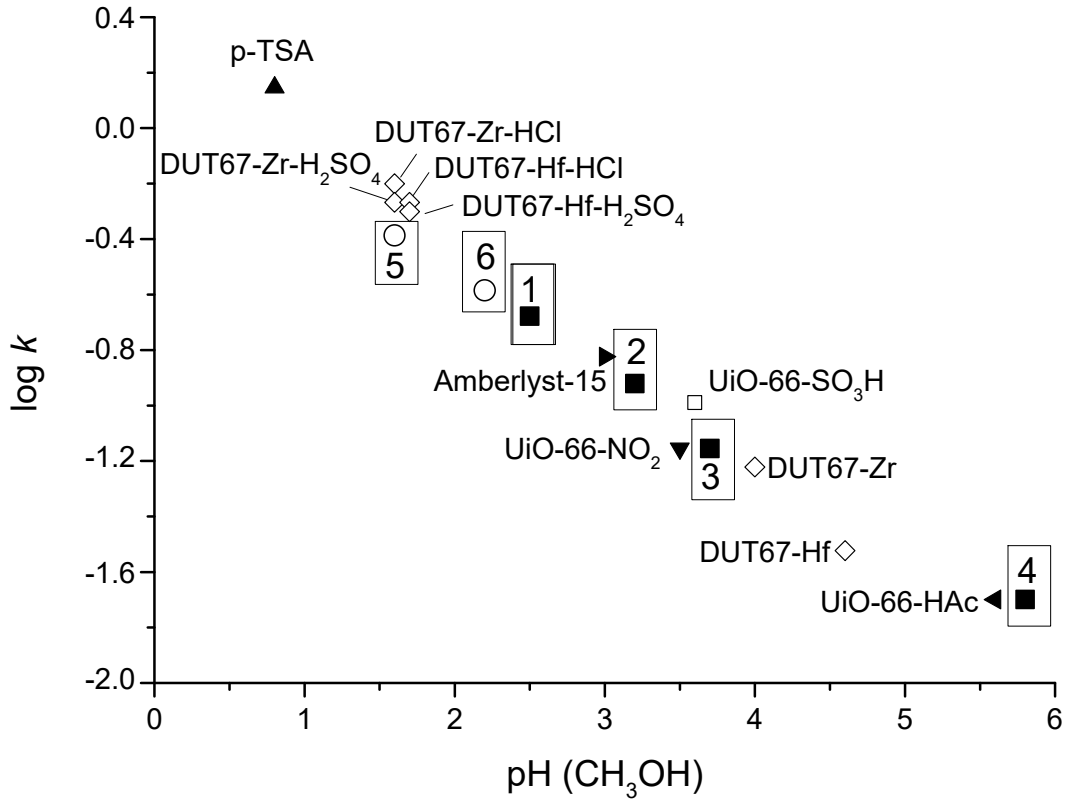
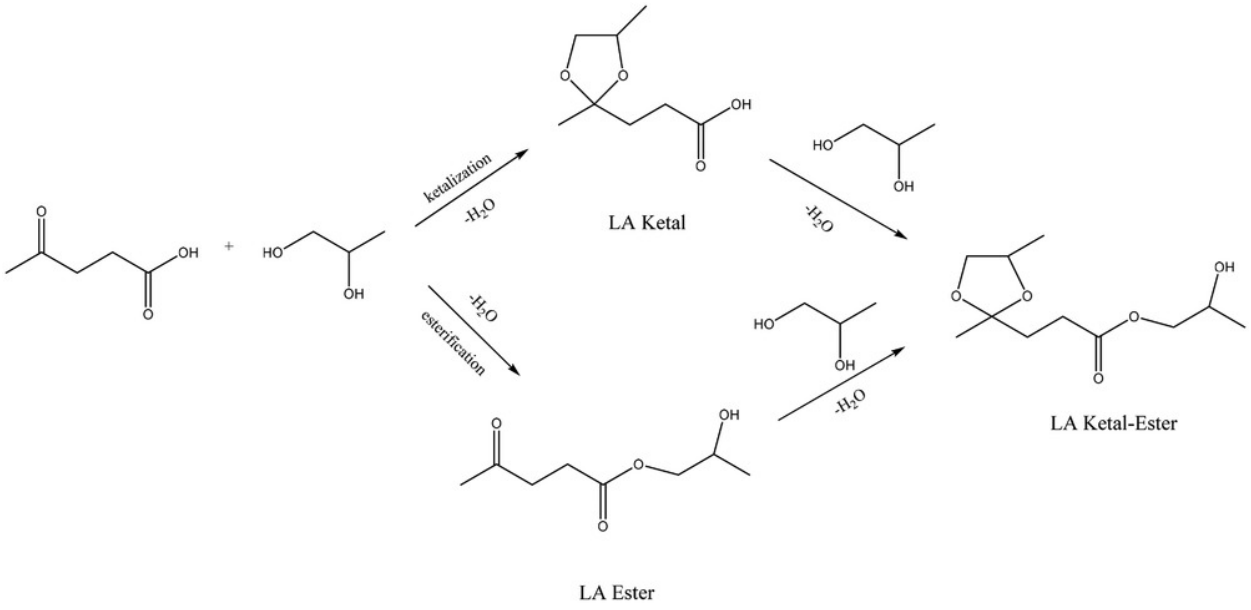


Figure 3. Logarithmic plot of the reaction rate constant of LA esterification (log *k*) versus the pH of a methanol dispersion of various catalysts, as indicated as follows: *para*-toluene sulfonic acid (▲); Amberlyst-15® (►); UiO-66-NO_2 (▼); UiO-66-HAc (◄); UiO-66-SO_3H (□); various Zr- and Hf-DUT-67 (◊). Samples of UiO-66 (■) and UiO-66-NH_2 (○) are numbered as follows. (1) Hydrated UiO-66 (7% of defects); (2) Dehydrated UiO-66 (7% of defects); (3) Hydrated UiO-66 (2% of defects); (4) Dehydrated UiO-66 (2% of defects); (5) Hydrated UiO-66-NH_2 (8.8% of defects); (6) Dehydrated UiO-66-NH_2 (8.8% of defects). Reproduced with permission from reference [22]. Copyright (2020) American Chemical Society.

5.1.3. Direct Ketalization of LA

Another reaction that effectively exploits the Brønsted-induced acidity of defective UiO-66 is the direct ketalization of LA. In this process, LA is reacted with a polyalcohol in the presence of an acid catalyst to form the corresponding ketal. Although seemingly a simple process, direct ketalization is complicated by the occurrence of the competing esterification of either the resulting levulinic ketal, or the starting LA, or both, thus yielding a mixture of products, namely ketal, ester, and ketal–ester, which lower the final yield of the desired ketal (see Scheme 5). For this reason, most of the reported studies on ketalization address the use of ethyl levulinate instead of LA to minimize competing (trans)esterification side reactions and to improve the final ketal selectivity [38–40]. Meanwhile, the direct ketalization of LA with various polyols was reported by Amarasekara and Animashaun over Amberlyst-15 and *p*-TSA catalysts [41]. Those authors concluded that selectivity to ketal depends on the catalyst structure and the number, nature, and accessibility of the active sites.



Scheme 5. Possible reaction routes of LA and 1,2-propanediol in the presence of an acid catalyst.

Given that the direct ketalization (and esterification) of LA is a largely unexplored reaction, we decided to test the effectivity of the Brønsted-induced acidity of defective UiO-66 for this reaction [42]. Our results showed that UiO-66 indeed catalyzes the direct ketalization of LA with 1,2-propanediol, achieving ketal selectivities over 90% at 90% conversion under optimized conditions. The results obtained depended on the alcohol excess used, thermal pre-activation of the catalyst, as well as the number of linker defects of UiO-66. This is clearly observed in Figure 4, where time–conversion plots of LA are shown for UiO-66 samples containing between 6 and 18% linker defects (part a). The calculated TOFs also increase linearly with the total number of defects of the catalyst, ranging from 9.2 to 20.3 h^{-1} from the least to the most defective materials (part b). Interestingly, the intrinsic activity per defective Zr^{4+} site was found to be roughly constant for all materials and around 68 $\pm$ 5 h^{-1} (part c), which demonstrates that all active sites are isolated and independent from one another, so that UiO-66 can be considered a true single-site catalyst [11]. Finally, it is also worth mentioning here that the activity of the other Zr-MOF considered in the present study, MOF-808, afforded a very limited activity for this reaction; only 35% LA conversion was achieved after 23 h of reaction, with an almost equal distribution of ester and ketal products and a very low TOF of 0.055 h^{-1}. This result was not unexpected, given the very weak character of the Brønsted acid sites in MOF-808, as discussed above in Section 3. This provides further proof that Brønsted acid sites are the true active sites for both esterification and ketalization reactions. On the other side of the scale, when a very strong Brønsted acid such as *p*-TSA was used as a catalyst, LA conversion was very fast (TOF = 56 h^{-1}), but the ketal selectivity was only 38%, with ketal–ester being the main reaction product. Similarly, Amberlyst-16, containing also strong sulfonic groups, afforded a good TOF of 36 h^{-1}, with an initially good selectivity to ketal at a short reaction time, but rapidly yielding the ester as the main reaction product. Taken together, all the results demonstrated that the nature and strength of the acid active sites strongly determine the final product distribution in this complex catalytic process. During the ketalization of LA and the esterification of both LA and the levulinic ketal formed in the first step, all reactions compete for the same active sites.

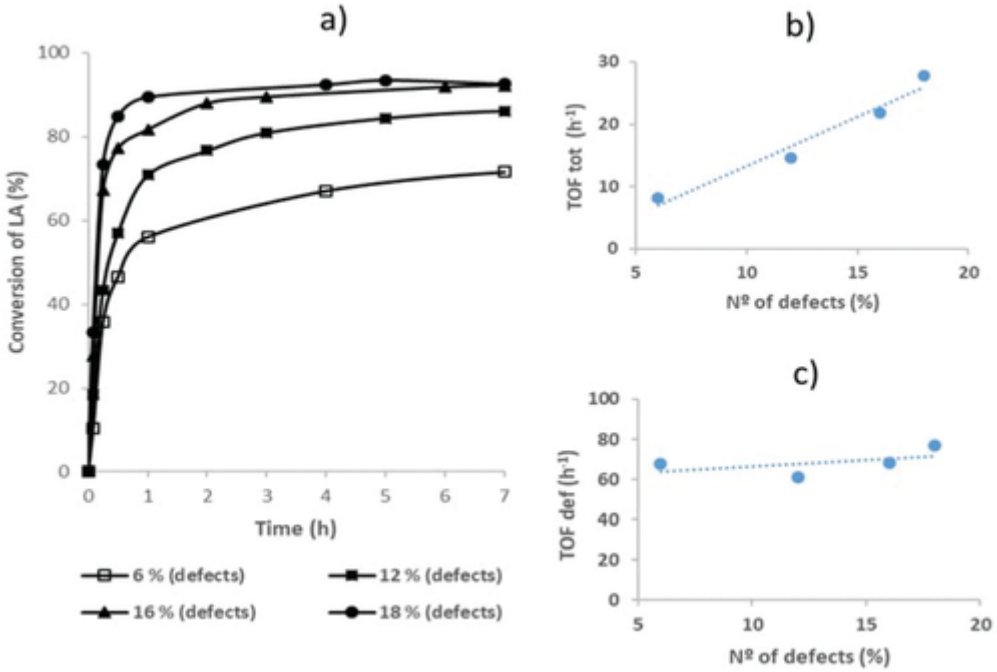
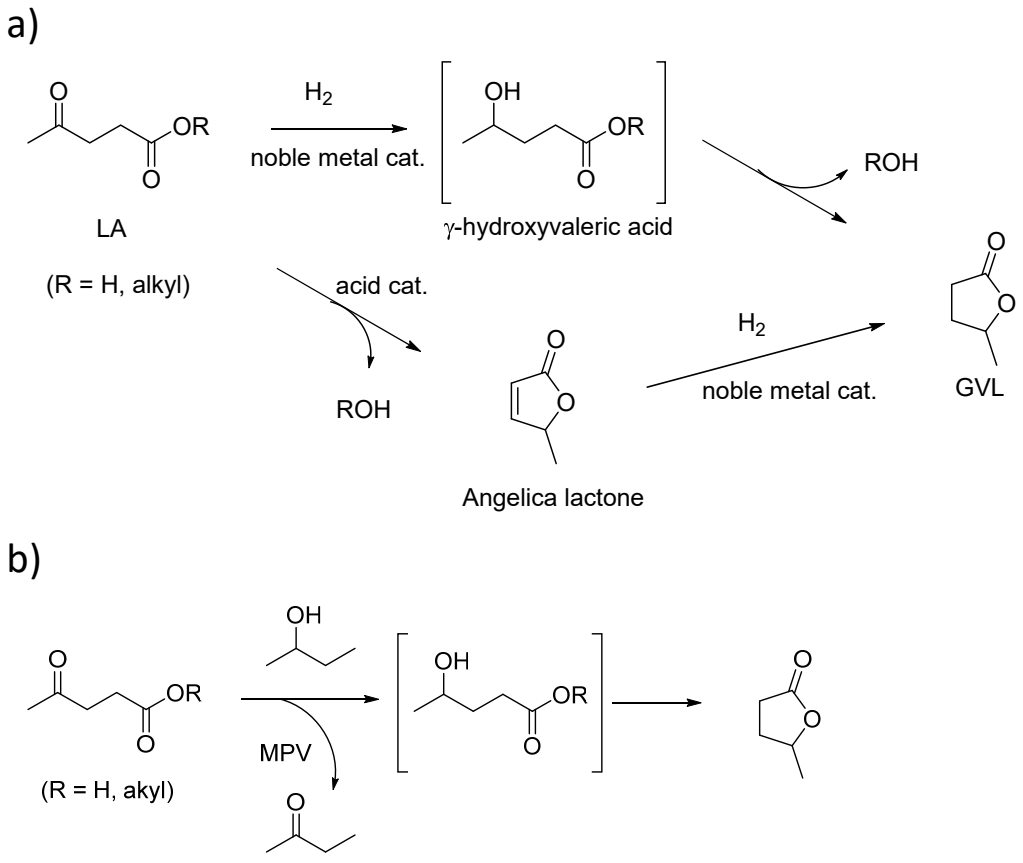


Figure 4. (**a**) Time–conversion plots of LA over various UiO-66 catalysts with different missing linker defects; (**b**) TOF_{tot}, calculated as mols of LA converted per total amount of Zr in the catalyst and per hour; and (**c**) TOF_{def}, calculated as mols of LA converted per amount of Zr associated with linker defects and per hour. Both TOF_{tot} and TOF_{def} are calculated at short reaction times (LA conversion lower than 30%). Reproduced from reference [42].

5.1.4. Synthesis of γ-Valerolactone (GVL)

LA conversion to GVL is usually achieved by one of the following two routes [43,44]: (i) the reduction of LA to γ-hydroxyvaleric acid followed by intramolecular cyclization and dehydration; and (ii) the dehydration of LA to angelica lactone catalyzed by acids and the hydrogenation of the C−C bond (Scheme 6). However, both routes use expensive noble metal catalysts and relatively high pressures (40–60 bar), and the water content of the LA feedstock used must be very low (<2.5 wt%) to avoid metal leaching and loss of catalytic activity. A third promising route has then been developed to overcome these limitations, consisting of a chemoselective reduction of the keto group of LA through a Meerwein–Ponndorf–Verley (MPV) catalytic transfer hydrogenation using a secondary alcohol as sacrificial source of hydrogen [45,46]. This route avoids the use of noble metal catalysts and the use of H_2 as a reducing agent. Both ZrO_2 [47] and Ni-Raney [48] were initially evaluated for this reaction. However, severe limitations were found, including the use of very elevated amounts of catalyst and sacrificial alcohol excess, and the process only worked smoothly when a levulinate ester was used as a starting product, but not directly from LA. Later, Zr- and Hf-beta zeolites [47,49–51] were used as catalysts for the MPV synthesis of GVL, starting either from LA or its esters. We then wanted to evaluate the potential of Zr MOFs as catalysts for this reaction. Indeed, de Vos and co-workers [52] first demonstrated the use of UiO-66 as an MPV catalyst for the conversion of geraniol with furfural, and later other Zr- and Hf-MOFs, such as MOF-808 [23,53–56] and DUT-67 [23], were successfully used as well. In particular, Valekar [56] and Rojas-Buzo [55] showed the use of Zr- and Hf-MOFs for the synthesis of GVL from ethyl levulinate, while we explored the direct synthesis from LA through various routes using UiO-66, MOF-808, and sulfated MOF-808 as catalysts [57].



Scheme 6. Synthesis of GVL from LA or its esters. (**a**) Acid–hydrogenation mechanisms; and (**b**) Meerwein–Ponndorf–Verley (MPV) catalytic transfer hydrogenation.

Valekar et al. [56] reported a maximum GVL yield of 92.7% after 2 h of reaction when ethyl levulinate (EL) was reacted with 2-propanol (IPA) in a 1:100 EL:IPA molar ratio at 200 °C in the presence of UiO-66. Meanwhile, MOF-808 was found to be the most active Zr-catalyst at 130 °C in terms of the GVL formation rate (94.4 mmol g^{-1} min^{-1}), which is very relevant for the discussion below. Rojas-Buzo et al. [55] reported the use of Hf-MOF-808 for the conversion of EL to GVL with IPA (~1:52 EL:IPA molar ratio), attaining a 94% yield after 8 h of reaction at 120 °C.

We explored different routes for converting LA into GVL [57]. The first route consisted of a two-step process in which LA was first esterified with *n*-butanol to *n*-buthyl levulinate (*n*BuL), and the results are shown in Figure 5 (data points before the vertical straight line in parts a–d) over UiO-66 (a), MOF-808 (b), and two sulfated MOF-808s with different degrees of sulfation (c and d). The sulfation process used was adapted from [58], as detailed in [57]. Once the esterification was completed, the resulting *n*BuL was reduced to GVL through a MPV reaction with *sec*-butanol (data points after the vertical line). Note that we used a primary alcohol in the first step to accelerate the esterification reaction, while a secondary alcohol was used to facilitate the ensuing MPV reaction. Obviously, the use of two different alcohols is not convenient from a practical point of view, but it is still useful from an academic point of view to evaluate the role of different types of acid sites in each individual step. Indeed, it is interesting to note here that, while the esterification and ketalization reactions commented above are both catalyzed by Brønsted acid sites only, the conversion of LA to GVL in two steps requires the simultaneous presence of two types of acid sites in the catalyst: Brønsted acid sites for the first esterification step and Lewis acid sites for the ensuing MPV step.

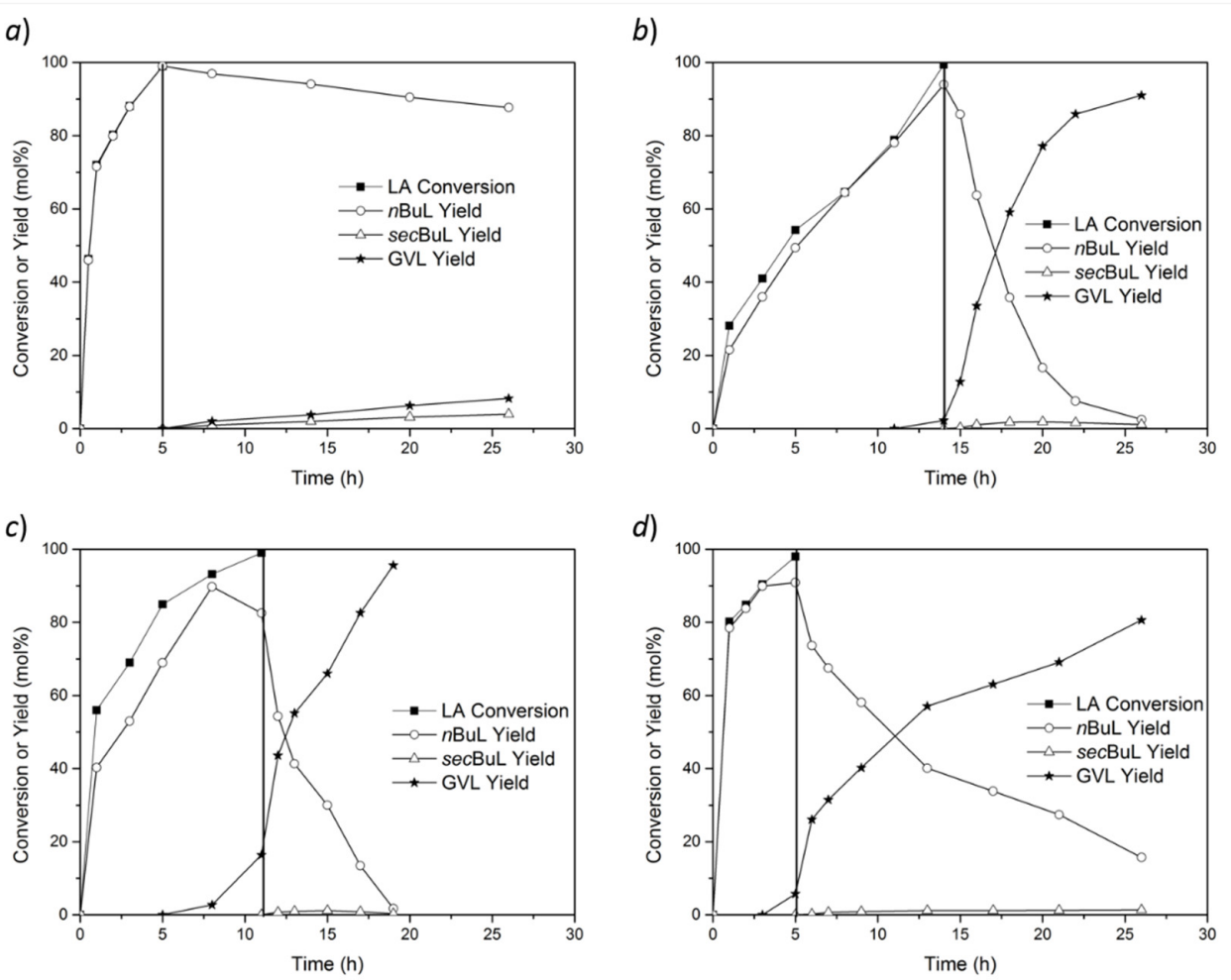


Figure 5. One-pot two-step conversion of LA over: (**a**) UiO-66; (**b**) MOF-808; (**c**) MOF-808-1.47SO_4; and (**d**) MOF-808-2.63SO_4. Vertical line indicates the end of the first step (esterification) and the addition of *sec*-BuOH to start the second step (MPV). Reproduced from reference [57].

As commented above, UiO-66 is a highly active catalyst for the esterification of LA, due to the presence of strong Brønsted-induced acid sites. As it can be observed in Figure 5a, LA is fully esterified to *n*BuL in 5 h. Conversely, the Brønsted acidity of MOF-808 is very weak. Therefore, the activity of MOF-808 for the esterification of LA with *n*BuOH was only moderate (Figure 5b). However, when MOF-808 was submitted to a sulfation process to increase the Brønsted acidity of the solid [58,59], the catalytic performance of the resulting MOF-808-SO_4 catalyst significantly improved. Thus, the time needed to achieve full LA esterification passed from 14 h for MOF-808 to 11 h and 5 h for two MOF-808-SO_4 samples with increasing sulfation degree (Figure 5c,d).

On the other hand, UiO-66 was not a good catalyst for the MPV reaction, which requires Lewis acid sites. The reasons for the poor performance of UiO-66 are two: (i) the small amount of Zr^{4+} Lewis sites in UiO-66, associated with missing linker defects; and (ii) the small pores of this MOF, which hinders the formation of the bulky transition state of the MPV reaction. In sharp contrast, MOF-808 has both a large amount of available Lewis sites (all Zr^{4+} centers can participate in the reaction) and much wider cavities to accommodate the sterically demanding transition state. Therefore, the catalytic activity of MOF-808 was much higher than UiO-66, as expected. Concerning sulfated MOF-808, the performance of the lowest sulfate sample was very good and comparable to pristine MOF-808, but it decreases somewhat for the deepest sulfated sample. This is probably due to the increasing

steric hindrance introduced by the sulfate groups in the MOF pores. Therefore, increasing the sulfation degree of MOF-808 has a positive effect on the first esterification step, but it does not compensate for the slowdown on the second MPV step. These results evidence the need to find the best equilibrium between Brønsted and Lewis acid sites in the solid catalyst to optimize the outcome of this multistep reaction.

6. Conversion of Lipids

6.1. Esterification of Free Fatty Acids (FFAs)

Biodiesel is a mixture of methyl and ethyl esters of long chain fatty acids (FAMEs or FAEEs) obtained from oils or fats (triglycerides), with properties similar to that of diesel obtained from oil (gasoil) [1,2]. However, compared with gasoil derived from petroleum, biodiesel has the main advantages of being biodegradable and it emits much fewer SO_x, CO, and solid particles when burnt in diesel engines. Therefore, biodiesel is considered to be less toxic than petroleum diesel. At the industrial scale, biodiesel is produced by the transesterification of tryglycerides using stoichiometric amounts of bases, such as sodium methoxide/potassium hydroxide. However, the triglycerides used as raw materials must have low water content to avoid catalyst neutralization or dilution, together with a low amount of free fatty acids to avoid saponification side reactions and the formation of emulsions, which complicate the separation of the target esters. Thus, the direct esterification of FFA with low molecular weight alcohols (methanol, ethanol) is an alternative route for preparing biodiesel compounds when raw materials with high FFA concentrations are used (such as wastes and byproducts coming from biomass processing plants or from food residues) [60]. This direct esterification of FFA with alcohols is usually carried out in the presence of an acid catalyst, such as sulfuric, phosphoric, hydrochloric, or organic sulfonic acids [61]. However, it is much preferred to develop new solid acid catalysts to allow the recovery of the catalyst, to facilitate the isolation of the target esters, and to reduce equipment corrosion associated with the use of mineral acids. As we will show throughout this section, metal–organic frameworks containing various metal cations (mainly Zr^{4+} or Hf^{4+}) have shown a high potential for this reaction.

While Chizallet et al. [62] and Savonnet et al. [63] described the transesterification of triglycerides or fatty esters using MOF catalysts, our group focused on the esterification of free fatty acids. We reported on the use of Zr-containing UiO-66 compounds, namely UiO-66 and UiO-66-NH_2, for the methanol and ethanol esterification reaction with a series of saturated fatty acids. These included saturated fatty acids with 12, 16, or 18 carbon atoms (C12 lauric acid; C16 palmitic acid; and C18 stearic acid), as well as unsaturated fatty acids with 18 carbon atoms (C18:1 oleic acid; C18:2 linoleic acid; and C18:3 α-linolenic acid) [64]. The results obtained in terms of the pseudo-first order rate constant are shown in Figure 6. In all the reactions studied, full acid conversion was achieved over UiO-66 and UiO-66-NH_2 and the ester was the only product detected. Moreover, both MOFs were found to be stable and reusable under the experimental conditions used. As can be observed in Figure 6, the reaction rate progressively decreases with the increase in the chain length and unsaturation degree of the fatty acid, which was attributed to a stronger adsorption of the reaction substrates or products on the catalyst surface and progressive deactivation of the acid centers [64]. Nevertheless, this deactivation is fully reversible and the catalysts recovered the initial activity by simply washing with ethanol.

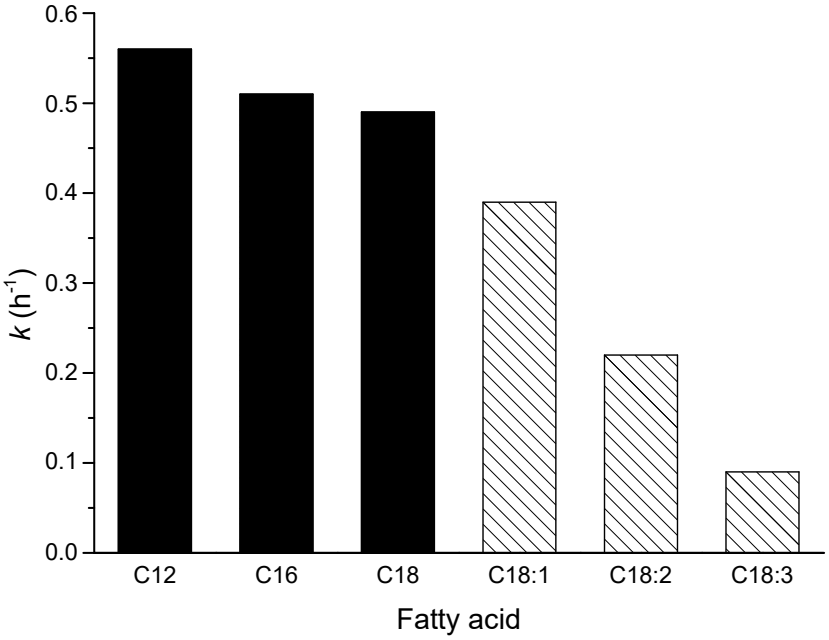
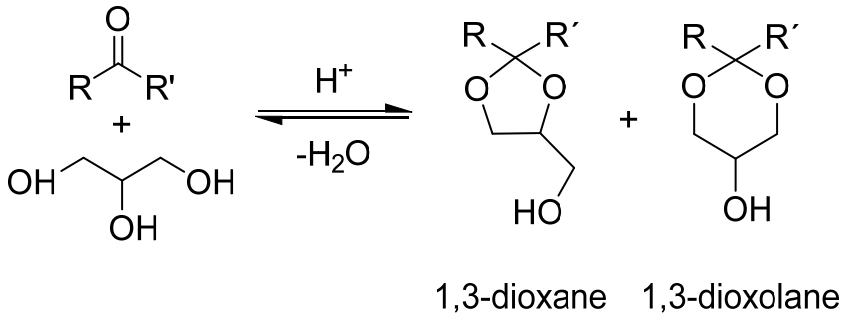


Figure 6. Pseudo-first order reaction rate constant (k) of esterification of saturated and unsaturated fatty acids with EtOH over UiO-66-NH_2.

6.2. Glycerol Valorization: Formation of Glyceryl Acetates

The increasing production of biodiesel in recent years has generated large stocks of glycerol, since this molecule is stoichiometrically formed from glyceride transesterification by 10 wt% of total biodiesel production [30]. Therefore, there is a great interest in developing novel routes for converting this largely abundant biodiesel by-product into commodity chemicals, such as reduction, oxidation, esterification, or acetalization, among others. In particular, glycerol reacts with carbonyl compounds to yield a mixture of 5- and 6-membered ring compounds, viz. 1,3-dioxan and 1,3-dioxolan, respectively, as shown in Scheme 7 [65–67]. The resulting glyceryl acetates find applications as fragrances [68], pharmaceutical products [69], surfactants [70], or fuel additives [66]. In this sense, we have recently reported on the use of Zr-UiO-66 as a heterogeneous catalyst for the synthesis of hyacinth and other glyceryl acetal fragrances [71].



Scheme 7. Glycerol acetalization produces a mixture of dioxane and dioxolane.

We have found that the catalytic activity of UiO-66 increases with the number of missing linker defects (see Figure 7), similar to the case of LA esterification discussed above. However, the intrinsic activity per defective Zr^{4+} site was roughly constant at a TOF around 350 h^{-1}, thus behaving as a single site catalyst. Interestingly, we found that the dioxolane–dioxane ratio in the final product can be adjusted between 2.8 and 4.6 by introducing -NH_2 in the MOF catalyst used and by controlling the amount of missing

linker defects. This affords a means to fine-tune the organoleptic characteristics of the final hyacinth fragrance mixture, which is highly desired for the fragrance industry.

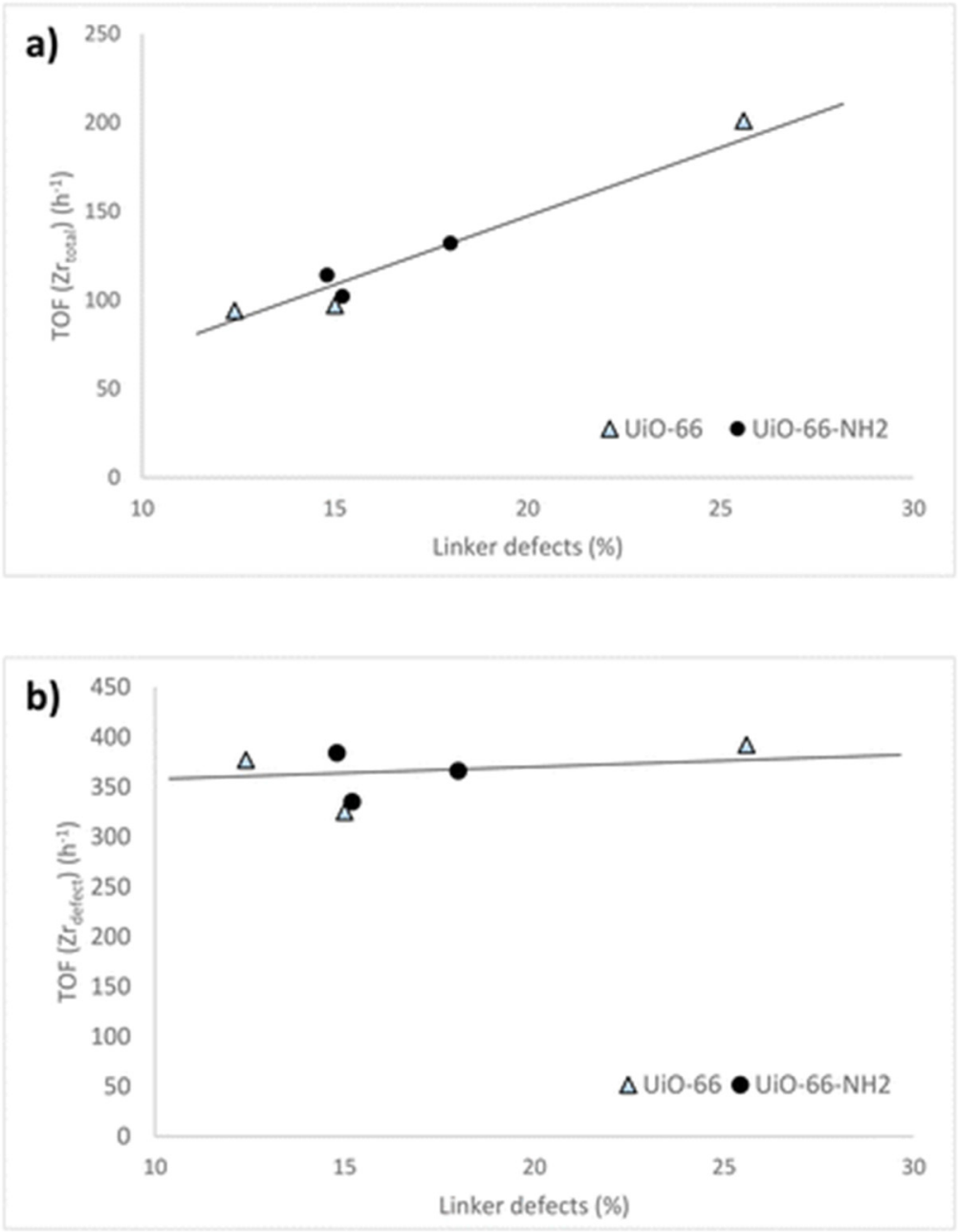
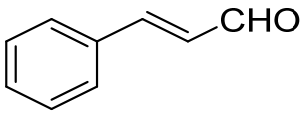
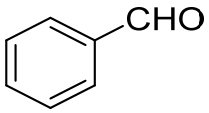
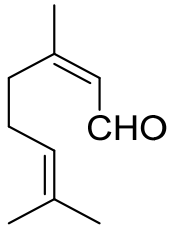
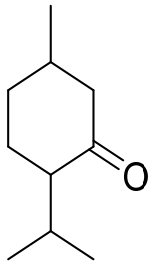
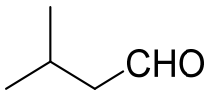
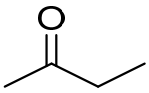


Figure 7. Turnover frequencies (TOFs) calculated for UiO-66 and UiO-66-NH_2 catalysts containing a variable amount of missing linker defects. In part (**a**), all the Zr in the catalyst is considered for TOF calculation, while in part (**b**), TOF is obtained only for Zr^{+4} sites associated with missing linker defects. Reproduced from reference [71].

Similar to the hyacinth fragrance, other acetals are indeed widely used in the fragrance industry, since acetalization can modify vapor pressure, aroma, and solubility of the starting aldehyde or ketone flavor. Interestingly, UiO-66 catalysts were also active for the acetalization of other carbonyl compounds, and the results obtained are summarized in Table 2.

Table 2. Acetalization of various carbonyl compounds with glycerol over UiO-66 [1].

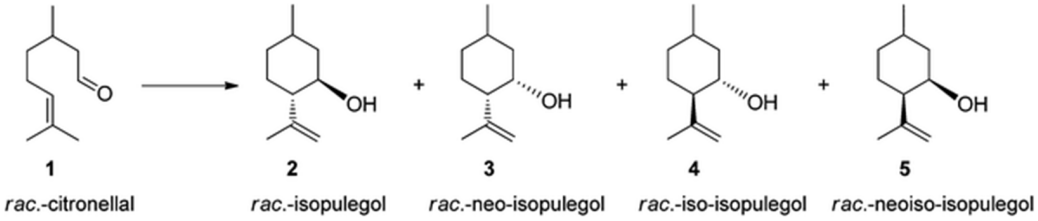
Carbonyl	Time (h)	Conv. (%)	Select. Dioxane (%)	Select. Dioxolane (%)
	3	100	57.8	42.2
	1	100	33.4	66.6
	3	100	60.9	39.1
	24	18.7	17.7	82.3
	3	99	30.5	69.5
	7	100	0	100

[1] Reaction conditions: aldehyde or ketone (1 mmol), glycerol (2 mmol), toluene (3 mL), UiO-66 (10 mg), Dean–Stark, 130 °C.

7. Conversion of Other Biomass-Derived Compounds

7.1. Isomerization of Terpenoids: Citronellal to Isopulegol Conversion

Menthol is a very important naturally occurring monoterpenoid compound largely used in the production of pharmaceuticals, agrochemicals, cosmetics, toothpastes, chewing gum, and other products. Natural (1*R*,2*S*,5*R*)−menthol is obtained from peppermint oil, but it is also manufactured by Takasago from myrcene [72]. An important step in this reaction is the carbonyl-ene isomerization of citronellal to isopulegol shown in Scheme 8, which is usually carried out catalytically using aqueous $ZnBr_2$ or tris(2,6-diarylphenoxy)aluminum catalysts. Citronellal can be converted into a mixture of four isomers, of which (-)-isopulegol is the target compound for the menthol synthesis. Therefore, several heterogeneous Lewis acid catalysts have been explored to improve the final stereoselectivity of the process.



Scheme 8. Carbonyl-ene isomerization of citronellal to isopulegol isomers. Isopulegol (2) is the target compound for the synthesis of (-)-menthol.

Alaerts et al. [73] first showed that the Cu^{2+} Lewis acid sites of copper trimesate MOF known as HKUST-1 can catalyze the isomerization reaction of various terpene derivatives, including α-pinene oxide to campholenic aldehyde and citronellal to isopulegol, as well as the rearrangement of the ethylene acetal of 2-bromopropiophenone. In the case of citronellal isomerization, the selectivity to (-)-isopulegol ranged between 65 and 69%. Later, we and others have shown that other MOFs can also catalyze this reaction, including Cr^{3+} in MIL-101 [74] or Zr^{4+} sites in UiO-66 [22,52] or MOF-808 [58].

The isomerization of citronellal is usually carried out in the presence of a Lewis acid catalyst, attaining high selectivities to the desired (-)-isopulegol isomer. However, clear differences are observed when the reaction is catalyzed by Brønsted acid sites. Isopulegol is still the major product obtained, but the final diastereoselectivity is considerably lower. This trend was clearly observed by comparing the catalytic activity of pristine and sulfated MOF-808 catalysts for this reaction. Pristine MOF-808 produced a very low citronellal conversion (only 8% conversion after 8 h of reaction), but a very high selectivity to isopulegol of 85%. Conversely, after the sulfation of MOF-808 to increase the Brønsted acidity of the catalyst, the activity increased considerably (98% citronellal conversion after 1.5 h of reaction time), but at the expense of isopulegol selectivity, which dropped to 55% [58].

As we have discussed above, UiO-66 type compounds provide a rare opportunity for tuning the Lewis/Brønsted acid properties by simply adjusting the hydration degree of the material, as depicted in Scheme 2. Accordingly, we explored the catalytic activity of hydrated and dehydrated UiO-66 containing 7% of missing linker defects for the citronellal isomerization, and the results obtained are shown in Figure 8. It is clearly observed that the catalytic activity of UiO-66 is higher for the dehydrated solid. Thus, the calculated rate constant of hydrated UiO-66 increases from 0.076 to 0.360 h^{-1} upon dehydration, i.e., an almost 5-fold increase. This higher activity for the dehydrated material versus hydrated UiO-66 indicates that Lewis acid sites catalyze the isomerization of citronellal more efficiently than Brønsted acid centers. Meanwhile, the selectivity to isopulegol also increases for dehydrated (Lewis acid) UiO-66, from 75% to 86%. The participation of the Zr^{4+} sites of UiO-66 in citronellal isomerization was also suggested by Vandichel et al. by using first-principle kinetic calculations [75]. Those authors concluded that Zr^{4+} would be present at defect positions, and they accordingly observed an increase in the catalytic activity with the number of linker defects [76]. Meanwhile, Brønsted acid centers in hydrated UiO-66 are not so effective, since the adsorption of citronellal onto Zr^{4+} sites must compete with strongly bound water molecules, resulting in a slowdown of the reaction.

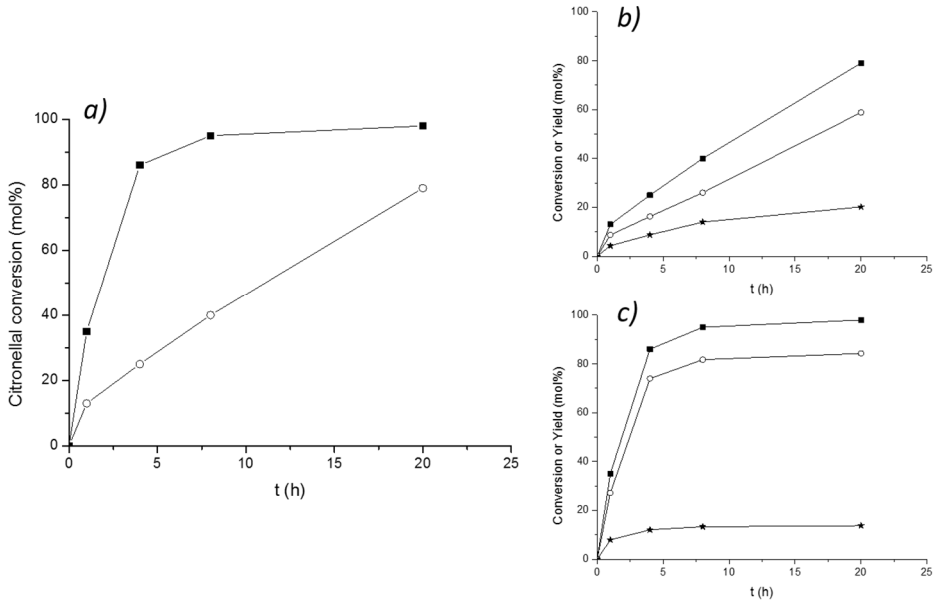
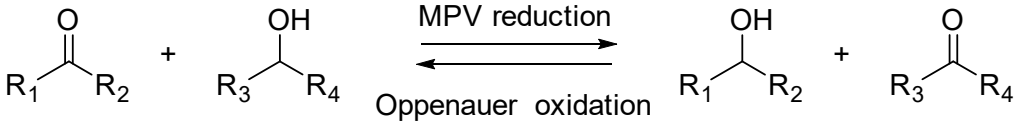


Figure 8. (**a**) Time–conversion plots of citronellal over hydrated (○) and dehydrated (■) UiO-66 with 7% of missing linker defects. Parts (**b**,**c**) show citronellal conversion (■) and yields to isopulegol (○) and other isopulegols (*) for hydrated (part (**b**)) and dehydrated (part (**c**)) UiO-66. Reproduced from reference [22].

7.2. Reduction of Carbonyl Compounds: Synthesis of Hydroxysteroids

One important route for the reduction of carbonyl compounds to the corresponding alcohol is the so-called Meerwein–Ponndorf–Verley (MPV) reaction using a secondary alcohol as a hydride source [77–79]. Interestingly, it can also be used in the opposite reaction, known as Oppenauer oxidation, to oxidize an alcohol with a sacrificial carbonyl compound, as shown in Scheme 9.



Scheme 9. MPVO transfer hydrogenation.

One main advantage of the MPVO reaction is that it is a chemoselective process. This means that the reaction can be carried out even with molecules containing other reducible functional groups besides the target carbonyl, such as conjugated and unconjugated unsaturated C–C bonds, esters, or nitro groups. This is not always the case with other existing methods for the reduction of carbonyls, such as direct hydrogenation with H_2 or reduction with other reducing agents, such as $NaBH_4$. In the case of the oxidation reaction (Oppenauer), no overoxidation to the carboxylic acid takes place. Another advantage of MPVO reactions is that they occur under mild conditions, which is highly desirable for the synthesis of natural products.

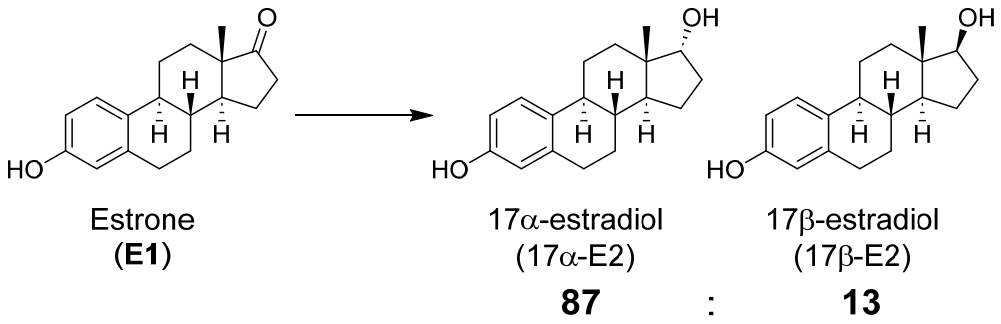
Various zirconium-containing MOFs have been successfully applied so far for MPVO reactions. Thus, Vermoortele et al. reported on the use of UiO-66-NO_2, the nitro analog of UiO-66, for the Oppenauer oxidation of geraniol with furfural [52]. Later, the same group demonstrated that the defects induced in UiO-66-NO_2 by treating the catalyst with HCl produced an enhancement of the catalytic activity of this material, UiO-66-NO_2-10_{HCl}, for the MPV reduction of *tert*-butylcyclohexanone with ^{i}PrOH compared to defective UiO-66-10_{HCl} [76]. Meanwhile, MOF-808 was also used for the MPV reduction of several α,β-unsaturated carbonyls, including the terpenoid *R*-carvone, using (*S*)-1-indanol as a

reducing agent [53]. We recently demonstrated the excellent performance of MOF-808 as a catalyst for the diastereoselective reduction of substituted cyclohexanones [23,80]. Also, as commented above, the reduction of levulinic acid or a levulinate ester can be carried out through a MPV reaction as well using MOF-808 as a catalyst [57]. In the following, we will describe in more detail an interesting use of MOF-808 as a heterogeneous catalyst for the reduction of ketosteroids to the corresponding hydroxysteroids.

As we have discussed above, UiO-66 has only a moderate activity for the MPV reaction. The reason for this limited performance is that only the Zr^{4+} ions at defect sites participate in the reaction. Additionally, the MPV reaction requires the formation of a bulky transition state, which can barely fit inside the reduced space of UiO-66 pores. Accordingly, we have shown that UiO-66 was a poor catalyst to reduce cyclohexanone to cyclohexanol through a MPV reaction with ^{i}PrOH as a hydride source; only 12% cyclohexanone conversion was attained after 1 h of reaction time [23]. On the other hand, all Zr^{4+} sites in MOF-808 can participate in the MPV reaction, and the pore cavities are much wider to accommodate the transition state. Therefore, a much higher cyclohexanone conversion was achieved under the same reaction conditions: 69% conversion after 1 h. And this activity improved further when defective sites were introduced by combining tritopic (trimesic acid) and ditopic ligands (isophthalic or pyridine dicarboxylic acid) during the synthesis of MOF-808; the conversion of cyclohexanone increased to 91 and 93% after 1 h, respectively.

Given the outstanding performance of MOF-808 and the large space available inside the pores, we then wanted to use it for converting very bulky substrates, such as substituted cyclohexanones [80] or estrone [23,81]. This is a natural steroid molecule with approximate dimensions of 11.2 Å × 6.2 Å × 4.2 Å. As expected, UiO-66 was completely inactive for the reduction of estrone (E1) to estradiol (E2), but both pristine and defect-engineered MOF-808 afforded the full conversion of E1 after 24 h of reaction.

The reduction of the (pro-chiral) carbonyl group of E1 at position 17 can give rise to a mixture of two estradiols: 17α-E2 and 17β-E2, as shown in Scheme 10.

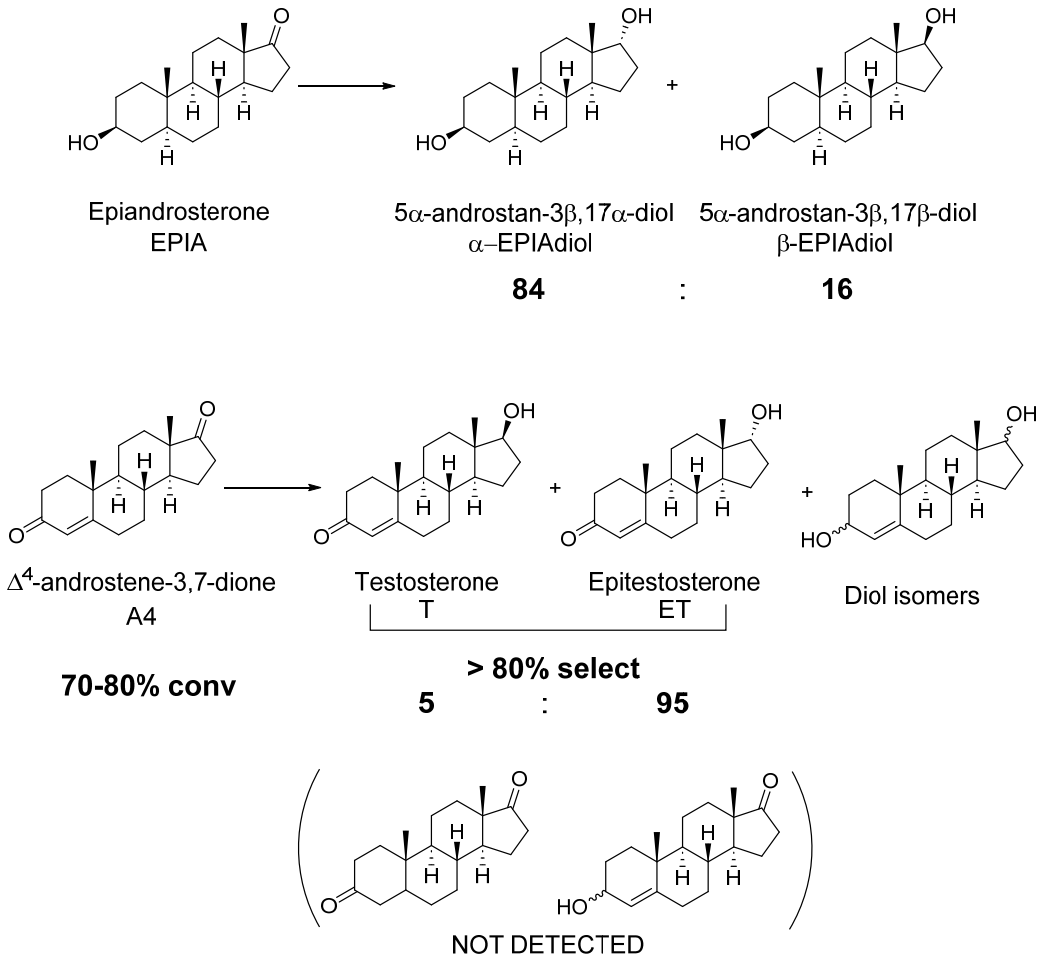


Scheme 10. Reduction of estrone (E1) yields a mixture of estradiols: 17α-E2 and 17β-E2 diastereoisomers.

Interestingly, when MOF-808 was used as an MPV catalyst for the reduction of E1, the main product obtained was 17α-E2, with a diastereoselectivity ratio of up to 87:13 under optimized conditions. It is worth noting that the formation of 17α-hydroxy steroids from the corresponding 17-ketosteroid is, in general, challenging. Usually, the 17β isomer is obtained almost exclusively when $NaBH_4$ or other reducing agents are used; the steric hindrance of the 18-methyl group imposes the approaching direction of the hydride from the *anti*-face, giving rise to $-CH_3$ and $-OH$ groups in *syn* configuration in the final product. Therefore, when 17α-OH compounds are the desired product, additional reactions are required to produce the inversion of the 17β-OH isomer through Mitsunobu reactions [82], involving multiple protection–deprotection steps and resulting in very low final yields. For example, Han et al. described the synthesis of a similar 17α-OH steroid (5α-androstane-3β,17α-diol)

from the 17-ketosteroid by a four-step reaction involving reduction, tosylation, acetate substitution, and hydrolysis, with a final yield of the 17α product of only 4% [83]. Ohta et al. introduced later a modification of this process by adding three more steps: epoxidation with peracetic acid, reduction with $NaBH_4$, and hydrolysis with NaOH, attaining a final yield of 54% [84]. Göndös and Orr used a chiral Rh complex, yielding the 17α-hydroxy-estrone-3-methyl ether in 36%, together with the 17β-compound in a 26% yield [85]. In sharp contrast with these poor results, the use of MOF-808 as an MPV catalyst affords a means for producing 17α-E2 in 87% selectivity in one single reaction step. Moreover, we showed that the solid catalyst can be easily recovered at the end of the reaction by simple filtration or centrifugation and used in consecutive catalytic runs without losing the activity of the diastereoselectivity to the elusive 17α-E2 compound for at least six catalytic cycles [81].

However, we wanted to go a step further and check if this remarkable diastereoselective synthesis of 17α-E2 could also be applied to the synthesis of other 17α-hydroxysteroids, as well as to address other important aspects of the reaction, such as the regio- and chemoselectivity of the MPV reduction of 17-ketosteroids over MOF-808. Scheme 11 summarizes the considered reactions and the results obtained.



Scheme 11. Summary of the results obtained in the MPV reduction of EPIA and A4 over MOF-808. See reference [81] for a detailed discussion.

Similar to E1, epiandrosterone (EPIA) also bears a keto group in position 17. When this molecule was submitted to a MPV reaction under the same conditions and using the MOF-808 catalyst, we also observed the formation of the 17α-OH compound as the main reaction product, thus evidencing the general applicability of the method. Moreover,

we then considered androstenedione (Δ^4-androstene-3,17-dione, A4) as a substrate. This compound contains two keto groups, in positions 3 and 17, as well as another easily reducible functional group, a C=C bond in position 4. Therefore, the use of A4 as a reaction substrate allowed us to evaluate the chemo- and regioselectivity of the MPV process using MOF-808 as a catalyst. To our delight, we observed the following: (i) the C=C bond in position 4 remains unaffected (100% chemoselectivity); (ii) no traces of monohydroxylated products in position 3 were detected (100% regioselectivity); (iii) reduction of the 17-keto group produces almost exclusively epitestosterone (ET), with a diastereoselectivity > 95%; and (iv) dihydroxylated products were only detected at high A4 conversions and long reaction times. Nevertheless, after optimization of the reaction conditions, we were still able to attain an A4 conversion of up to 70–80% while maintaining an excellent selectivity higher than 80% to the monohydroxylated product in position 17, forming ET almost exclusively.

In order to understand the excellent results obtained for the MPV reduction of 17-ketosteroids to the challenging 17α-OH derivatives over MOF-808, we performed temperature-dependent kinetic analysis to evaluate the reaction rate constants of E1 reduction with ^{i}PrOH and 2-BuOH. The apparent activation energies and the corresponding thermodynamic parameters were derived from the corresponding Arrhenius and Eyring–Polanyi equations. The analysis of the energy differences between the two transition states leading to 17α-E2 and 17β-E2 revealed a dominant contribution from the entropic term when 2-BuOH was used as a hydride source, while the entropic and enthalpic terms partially neutralize each other when ^{i}PrOH is used, resulting in a lower diastereoselectivity [81]. These findings suggest that the selectivity to the 17α isomer originates from the confinement of the reaction inside the MOF cavities, where Zr^{4+} sites are located.

8. Conclusions

In this work, we have reviewed illustrative examples that demonstrate the great potential of Zr^{4+} MOFs UiO-66 and MOF-808 as heterogeneous catalysts for the conversion of biomass-derived compounds into valuable chemicals. Despite the many similarities existing between these two Zr-MOFs, such as the presence of $Zr_6O_4(OH)_4$ oxoclusters, their chemical properties are very different in terms of Brønsted/Lewis characteristics, and they depend upon (i) the number of missing linker point defects (in UiO-66) and (ii) the hydration state of the solid at the beginning of the reaction. By adjusting these two important parameters, we have shown that it is possible to shift easily from a Brønsted acid to a Lewis acid, which adds a new dimension in the design and engineering of MOFs for catalytic applications. Thus, depending on the reaction that we want to address and the nature of the acid sites required to catalyze it, it is preferable to use one or the other catalyst.

In this review, we have limited ourselves to consider only example reactions in which UiO-66 and MOF-808 compounds are used for the conversion of biomass compounds. However, it is worth recalling that these materials have been successfully used as heterogeneous catalysts for many other reactions, including the synthesis of fine chemicals [11]. Moreover, the reported examples are not just limited to Zr-containing compounds, since these materials can be readily obtained with other tetravalent ions such as Hf, Ce, or Ti [16,55,86,87]. This provides additional tools for finely tuning the catalytic properties of the solid, such as the hardness/softness of the Lewis acid sites, Brønsted acid strength, or their redox properties. To this, it has to be added the possibility to modify the organic linkers to include additional functional groups that can participate directly in the catalytic reaction or they can modify the acid strength of the metal ions through electronic effects [52]. Altogether, the possibilities to change the chemical composition and properties are almost endless, which convert these MOFs into excellent platforms for evaluating structure-composition-activity relationships.

Funding: Financial support from the Spanish Ministry of Science and Innovation (PID2020-112590GB-C21, PID2023-146114NB-C21, and CEX2021-001230-S grants funded by MCIN/AEI/10.13039/501100011033) is gratefully acknowledged. This study forms part of the Advanced Materials Program and was supported by MICIN with funding from European Union NextGeneration (PRTR-C17.I1) and by the Generalitat Valenciana (MFA/2022/003).

Conflicts of Interest: The authors declare no conflicts of interest.

References

1. Huber, G.W.; Iborra, S.; Corma, A. Synthesis of Transportation Fuels from Biomass: Chemistry, Catalysts, and Engineering. *Chem. Rev.* **2006**, *106*, 4044–4098. [CrossRef] [PubMed]
2. Corma Canos, A.; Iborra, S.; Velty, A. Chemical Routes for the Transformation of Biomass into Chemicals. *Chem. Rev.* **2007**, *107*, 2411–2502. [CrossRef] [PubMed]
3. Bozell, J.J.; Petersen, G.R. Technology Development for the Production of Biobased Products from Biorefinery Carbohydrates—The US Department of Energy's "Top 10" Revisited. *Green Chem.* **2010**, *12*, 539–554. [CrossRef]
4. Rowsell, J.L.C.; Yaghi, O.M. Metal-Organic Frameworks: A New Class of Porous Materials. *Microporous Mesoporous Mater.* **2004**, *73*, 3–14. [CrossRef]
5. Rosi, N.L.; Eddaoudi, M.; Kim, J.; O'Keeffe, M.; Yaghi, O.M. Advances in the Chemistry of Metal–Organic Frameworks. *CrystEngComm* **2002**, *4*, 401–404. [CrossRef]
6. Tranchemontagne, D.J.; Mendoza-Cortés, J.L.; O'Keeffe, M.; Yaghi, O.M. Secondary Building Units, Nets and Bonding in the Chemistry of Metal-Organic Frameworks. *Chem. Soc. Rev.* **2009**, *38*, 1257–1283. [CrossRef]
7. Farha, O.K.; Eryazici, I.; Jeong, N.C.; Hauser, B.G.; Wilmer, C.E.; Sarjeant, A.A.; Snurr, R.Q.; Nguyen, S.T.; Yazaydin, A.O.; Hupp, J.T. Metal–Organic Framework Materials with Ultrahigh Surface Areas: Is the Sky the Limit? *J. Am. Chem. Soc.* **2012**, *134*, 15016–15021. [CrossRef]
8. Hönicke, I.M.; Senkovska, I.; Bon, V.; Baburin, I.A.; Bönisch, N.; Raschke, S.; Evans, J.D.; Kaskel, S. Balancing Mechanical Stability and Ultrahigh Porosity in Crystalline Framework Materials. *Angew. Chem. Int. Ed.* **2018**, *57*, 13780–13783. [CrossRef]
9. Corma, A.; Garcia, H.; Llabrés i Xamena, F.X. Engineering Metal Organic Frameworks for Catalysis. *Chem. Rev.* **2010**, *110*, 4606–4655. [CrossRef]
10. Gascon, J.; Corma, A.; Kapteijn, F.; Llabrés i Xamena, F.X. Metal Organic Framework Catalysis: Quo Vadis? *ACS Catal.* **2014**, *4*, 361–378. [CrossRef]
11. Rogge, S.M.J.; Bavykina, A.; Hajek, J.; Garcia, H.; Olivos-Suarez, A.I.; Sepúlveda-Escribano, A.; Vimont, A.; Clet, G.; Bazin, P.; Kapteijn, F.; et al. Metal–Organic and Covalent Organic Frameworks as Single-Site Catalysts. *Chem. Soc. Rev.* **2017**, *46*, 3134–3184. [CrossRef] [PubMed]
12. Cavka, J.H.; Jakobsen, S.; Olsbye, U.; Guillou, N.; Lamberti, C.; Bordiga, S.; Lillerud, K.P. A New Zirconium Inorganic Building Brick Forming Metal Organic Frameworks with Exceptional Stability. *J. Am. Chem. Soc.* **2008**, *130*, 13850–13851. [CrossRef] [PubMed]
13. Furukawa, H.; Gándara, F.; Zhang, Y.B.; Jiang, J.; Queen, W.L.; Hudson, M.R.; Yaghi, O.M. Water Adsorption in Porous Metal-Organic Frameworks and Related Materials. *J. Am. Chem. Soc.* **2014**, *136*, 4369–4381. [CrossRef]
14. Wu, H.; Yildirim, T.; Zhou, W. Exceptional Mechanical Stability of Highly Porous Zirconium Metal–Organic Framework UiO-66 and Its Important Implications. *J. Phys. Chem. Lett.* **2013**, *4*, 925–930. [CrossRef]
15. Jakobsen, S.; Gianolio, D.; Wragg, D.S.; Nilsen, M.H.; Emerich, H.; Bordiga, S.; Lamberti, C.; Olsbye, U.; Tilset, M.; Lillerud, K.P. Structural Determination of a Highly Stable Metal-Organic Framework with Possible Application to Interim Radioactive Waste Scavenging: Hf-UiO-66. *Phys. Rev. B Condens. Matter Mater. Phys.* **2012**, *86*, 125429. [CrossRef]
16. Lammert, M.; Wharmby, M.T.; Smolders, S.; Bueken, B.; Lieb, A.; Lomachenko, K.A.; De Vos, D.; Stock, N. Cerium-Based Metal Organic Frameworks with UiO-66 Architecture: Synthesis, Properties and Redox Catalytic Activity. *Chem. Commun.* **2015**, *51*, 12578–12581. [CrossRef]
17. Smith, S.J.D.; Ladewig, B.P.; Hill, A.J.; Lau, C.H.; Hill, M.R. Post-Synthetic Ti Exchanged UiO-66 Metal-Organic Frameworks That Deliver Exceptional Gas Permeability in Mixed Matrix Membranes. *Sci. Rep.* **2015**, *5*, 7823. [CrossRef]
18. Bai, Y.; Dou, Y.; Xie, L.H.; Rutledge, W.; Li, J.R.; Zhou, H.C. Zr-Based Metal–Organic Frameworks: Design, Synthesis, Structure, and Applications. *Chem. Soc. Rev.* **2016**, *45*, 2327–2367. [CrossRef]
19. Schaate, A.; Roy, P.; Preuße, T.; Lohmeier, S.J.; Godt, A.; Behrens, P. Porous Interpenetrated Zirconium–Organic Frameworks (PIZOFs): A Chemically Versatile Family of Metal–Organic Frameworks. *Chem.-A Eur. J.* **2011**, *17*, 9320–9325. [CrossRef]
20. Cirujano, F.G.; Corma, A.; Llabrés i Xamena, F.X. Conversion of Levulinic Acid into Chemicals: Synthesis of Biomass Derived Levulinate Esters over Zr-Containing MOFs. *Chem. Eng. Sci.* **2015**, *124*, 52–60. [CrossRef]

21. Shearer, G.C.; Chavan, S.; Bordiga, S.; Svelle, S.; Olsbye, U.; Petter Lillerud, K. Defect Engineering: Tuning the Porosity and Composition of the Metal–Organic Framework UiO-66 via Modulated Synthesis. *Chem. Mater.* **2016**, *28*, 3749–3761. [CrossRef]
22. Cirujano, F.G.; Llabrés i Xamena, F.X. Tuning the Catalytic Properties of UiO-66 Metal-Organic Frameworks: From Lewis to Defect-Induced Brønsted Acidity. *J. Phys. Chem. Lett.* **2020**, *11*, 4879–4890. [CrossRef] [PubMed]
23. Mautschke, H.-H.; Drache, F.; Senkovska, I.; Kaskel, S.; Llabrés i Xamena, F.X. Catalytic Properties of Pristine and Defect-Engineered Zr-MOF-808 Metal Organic Frameworks. *Catal. Sci. Technol.* **2018**, *8*, 3610–3616. [CrossRef]
24. Zhang, J.; Wu, S.; Li, B.; Zhang, H. Advances in the Catalytic Production of Valuable Levulinic Acid Derivatives. *ChemCatChem* **2012**, *4*, 1230–1237. [CrossRef]
25. Hayes, D.J. An Examination of Biorefining Processes, Catalysts and Challenges. *Catal. Today* **2009**, *145*, 138–151. [CrossRef]
26. Allaoua, I.; Goi, B.E.; Obadia, M.M.; Debuigne, A.; Detrembleur, C.; Drockenmuller, E. (Co)Polymerization of Vinyl Levulinate by Cobalt-Mediated Radical Polymerization and Functionalization by Ketoxime Click Chemistry. *Polym. Chem.* **2014**, *5*, 2973–2979. [CrossRef]
27. Sinisi, A.; Degli Esposti, M.; Toselli, M.; Morselli, D.; Fabbri, P. Biobased Ketal-Diester Additives Derived from Levulinic Acid: Synthesis and Effect on the Thermal Stability and Thermo-Mechanical Properties of Poly(Vinyl Chloride). *ACS Sustain. Chem. Eng.* **2019**, *7*, 13920–13931. [CrossRef]
28. Mallesham, B.; Govinda Rao, B.; Reddy, B.M. Production of Biofuel Additives by Esterification and Acetalization of Bioglycerol. *Comptes Rendus Chim.* **2016**, *19*, 1194–1202. [CrossRef]
29. Xuan, W.; Hakkarainen, M.; Odelius, K. Levulinic Acid as a Versatile Building Block for Plasticizer Design. *ACS Sustain. Chem. Eng.* **2019**, *7*, 12552–12562. [CrossRef]
30. Climent, M.J.; Corma, A.; Iborra, S. Conversion of Biomass Platform Molecules into Fuel Additives and Liquid Hydrocarbon Fuels. *Green Chem.* **2014**, *16*, 516–547. [CrossRef]
31. Horváth, I.T.; Mehdi, H.; Fábos, V.; Boda, L.; Mika, L.T. γ-Valerolactone—A Sustainable Liquid for Energy and Carbon-Based Chemicals. *Green Chem.* **2008**, *10*, 238–242. [CrossRef]
32. Fegyverneki, D.; Orha, L.; Láng, G.; Horváth, I.T. Gamma-Valerolactone-Based Solvents. *Tetrahedron* **2010**, *66*, 1078–1081. [CrossRef]
33. Palkovits, R. Pentenoic Acid Pathways for Cellulosic Biofuels. *Angew. Chem.—Int. Ed.* **2010**, *49*, 4336–4338. [CrossRef] [PubMed]
34. Lange, J.P.; Price, R.; Ayoub, P.M.; Louis, J.; Petrus, L.; Clarke, L.; Gosselink, H. Valeric Biofuels: A Platform of Cellulosic Transportation Fuels. *Angew. Chem.—Int. Ed.* **2010**, *49*, 4479–4483. [CrossRef] [PubMed]
35. Serrano-Ruiz, J.C.; Wang, D.; Dumesic, J.A. Catalytic Upgrading of Levulinic Acid to 5-Nonanone. *Green Chem.* **2010**, *12*, 574–577. [CrossRef]
36. Caratelli, C.; Hajek, J.; Cirujano, F.G.; Waroquier, M.; Llabrés i Xamena, F.X.; Van Speybroeck, V. Nature of Active Sites on UiO-66 and Beneficial Influence of Water in the Catalysis of Fischer Esterification. *J. Catal.* **2017**, *352*, 401–414. [CrossRef]
37. Valenzano, L.; Civalleri, B.; Chavan, S.; Bordiga, S.; Nilsen, M.H.; Jakobsen, S.; Lillerud, K.P.; Lamberti, C. Disclosing the Complex Structure of UiO-66 Metal Organic Framework: A Synergic Combination of Experiment and Theory. *Chem. Mater.* **2011**, *23*, 1700–1718. [CrossRef]
38. Freitas, F.A.; Licursi, D.; Lachter, E.R.; Galletti, A.M.R.; Antonetti, C.; Brito, T.C.; Nascimento, R.S.V. Heterogeneous Catalysis for the Ketalisation of Ethyl Levulinate with 1,2-Dodecanediol: Opening the Way to a New Class of Bio-Degradable Surfactants. *Catal. Commun.* **2016**, *73*, 84–87. [CrossRef]
39. Selifonov, S.; Rothstein, S.D.; Mullen, B.D. Method of Making Ketals and Acetals. U.S. Patent US8604223B22013, 10 December 2013.
40. Mullen, B.D.; Badarinarayana, V.; Santos-Martinez, M.; Selifonov, S. Catalytic Selectivity of Ketalization versus Transesterification. *Top. Catal.* **2010**, *53*, 1235–1240. [CrossRef]
41. Amarasekara, A.S.; Animashaun, M.A. Acid Catalyzed Competitive Esterification and Ketalization of Levulinic Acid with 1,2 and 1,3-Diols: The Effect of Heterogeneous and Homogeneous Catalysts. *Catal. Lett.* **2016**, *146*, 1819–1824. [CrossRef]
42. Rapeyko, A.; Rodenas, M.; Llabrés i Xamena, F.X. Zr-Containing UiO-66 Metal-Organic Frameworks as Highly Selective Heterogeneous Acid Catalysts for the Direct Ketalization of Levulinic Acid. *Adv. Sustain. Syst.* **2022**, *6*, 2100451. [CrossRef]
43. Serrano-Ruiz, J.C.; West, R.M.; Dumesic, J.A. Catalytic Conversion of Renewable Biomass Resources to Fuels and Chemicals. *Annu. Rev. Chem. Biomol. Eng.* **2010**, *1*, 79–100. [CrossRef] [PubMed]
44. Wright, W.R.H.; Palkovits, R. Development of Heterogeneous Catalysts for the Conversion of Levulinic Acid to γ-Valerolactone. *ChemSusChem* **2012**, *5*, 1657–1667. [CrossRef] [PubMed]
45. Antunes, M.M.; Silva, A.F.; Fernandes, A.; Valente, A.A. γ-Valerolactone Synthesis from α-Angelica Lactone and Levulinic Acid over Biobased Multifunctional Nanohybrid Catalysts. *Catal. Today* **2021**, *in press*. [CrossRef]
46. Xu, C.; Paone, E.; Rodrí Guez-Padró, D.; Luque, R.; Mauriello, F. Recent Catalytic Routes for the Preparation and the Upgrading of Biomass Derived Furfural and 5-Hydroxymethylfurfural. *Chem. Soc. Rev.* **2020**, *49*, 4273. [CrossRef]

47. Chia, M.; Dumesic, J.A. Liquid-Phase Catalytic Transfer Hydrogenation and Cyclization of Levulinic Acid and Its Esters to γ-Valerolactone over Metal Oxide Catalysts. *Chem. Commun.* **2011**, *47*, 12233–12235. [CrossRef]
48. Yang, Z.; Huang, Y.B.; Guo, Q.X.; Fu, Y. Raney® Ni Catalyzed Transfer Hydrogenation of Levulinate Esters to γ-Valerolactone at Room Temperature. *Chem. Commun.* **2013**, *49*, 5328–5330. [CrossRef]
49. Luo, H.Y.; Consoli, D.F.; Gunther, W.R.; Román-Leshkov, Y. Investigation of the Reaction Kinetics of Isolated Lewis Acid Sites in Beta Zeolites for the Meerwein–Ponndorf–Verley Reduction of Methyl Levulinate to g-Valerolactone. *J. Catal.* **2014**, *32*, 198–207. [CrossRef]
50. Bui, L.; Luo, H.; Gunther, W.R.; Román-Leshkov, Y. Domino Reaction Catalyzed by Zeolites with Brønsted and Lewis Acid Sites for the Production of G-Valerolactone from Furfural. *Angew. Chem.—Int. Ed.* **2013**, *52*, 8180–8183. [CrossRef]
51. Wang, J.; Jaenicke, S.; Chuah, G.K. Zirconium–Beta Zeolite as a Robust Catalyst for the Transformation of Levulinic Acid to g-Valerolactone via Meerwein–Ponndorf–Verley Reduction. *RSC Adv.* **2014**, *4*, 13481–13489. [CrossRef]
52. Vermoortele, F.; Vandichel, M.; Van de Voorde, B.; Ameloot, R.; Waroquier, M.; Van Speybroeck, V.; de Vos, D.E. Electronic Effects of Linker Substitution on Lewis Acid Catalysis with Metal–Organic Frameworks. *Angew. Chem. Int. Ed.* **2012**, *51*, 4887–4890. [CrossRef]
53. Plessers, E.; Fu, G.; Tan, C.Y.X.; de Vos, D.E.; Roeffaers, M.B.J. Zr-Based MOF-808 as Meerwein–Ponndorf–Verley Reduction Catalyst for Challenging Carbonyl Compounds. *Catalysts* **2016**, *6*, 104. [CrossRef]
54. Valekar, A.H.; Lee, M.; Yoon, J.W.; Kwak, J.; Hong, D.Y.; Oh, K.R.; Cha, G.Y.; Kwon, Y.U.; Jung, J.; Chang, J.S.; et al. Catalytic Transfer Hydrogenation of Furfural to Furfuryl Alcohol under Mild Conditions over Zr-MOFs: Exploring the Role of Metal Node Coordination and Modification. *ACS Catal.* **2020**, *10*, 3720–3732. [CrossRef]
55. Rojas-Buzo, S.; Garcia-Garcia, P.; Corma, A. Catalytic Transfer Hydrogenation of Biomass-Derived Carbonyls over Hafnium-Based Metal–Organic Frameworks. *ChemSusChem* **2018**, *11*, 432–438. [CrossRef]
56. Valekar, A.H.; Cho, K.-H.; Chitale, S.K.; Hong, D.-Y.; Cha, G.-Y.; Lee, U.-H.; Hwang, D.W.; Serre, C.; Chang, J.-S.; Hwang, Y.K. Catalytic Transfer Hydrogenation of Ethyl Levulinate to γ-Valerolactone over Zirconium-Based Metal–Organic Frameworks. *Green Chem.* **2016**, *18*, 4542–4552. [CrossRef]
57. Guarinos, J.M.; Cirujano, F.G.; Rapeyko, A.; Llabrés i Xamena, F.X. Conversion of Levulinic Acid to γ-Valerolactone over Zr-Containing Metal-Organic Frameworks: Evidencing the Role of Lewis and Brønsted Acid Sites. *Mol. Catal.* **2021**, *515*, 111925. [CrossRef]
58. Jiang, J.; Gándara, F.; Zhang, Y.-B.; Na, K.; Yaghi, O.M.; Klemperer, W.G. Superacidity in Sulfated Metal−Organic Framework-808. *J. Am. Chem. Soc.* **2014**, *136*, 12844–12847. [CrossRef]
59. Trickett, C.A.; Popp, T.M.O.; Su, J.; Yan, C.; Weisberg, J.; Huq, A.; Urban, P.; Jiang, J.; Kalmutzki, M.J.; Liu, Q.; et al. Identification of the Strong Brønsted Acid Site in a Metal–Organic Framework Solid Acid Catalyst. *Nat. Chem.* **2019**, *11*, 170–176. [CrossRef]
60. Vieira, S.S.; Magriotis, Z.M.; Santos, N.A.V.; Saczk, A.A.; Hori, C.E.; Arroyo, P.A. Biodiesel Production by Free Fatty Acid Esterification Using Lanthanum (La^{3+}) and HZSM-5 Based Catalysts. *Bioresour. Technol.* **2013**, *133*, 248–255. [CrossRef]
61. Ma, F.; Hanna, M.A. Biodiesel Production: A Review. *Bioresour. Technol.* **1999**, *70*, 1–15. [CrossRef]
62. Chizallet, C.; Lazare, S.; Bazer-Bachi, D.; Bonnier, F.; Lecocq, V.; Soyer, E.; Quoineaud, A.A.; Bats, N. Catalysis of Transesterification by a Nonfunctionalized Metal-Organic Framework: Acido-Basicity at the External Surface of ZIF-8 Probed by FTIR and Ab Initio Calculations. *J. Am. Chem. Soc.* **2010**, *132*, 12365–12377. [CrossRef]
63. Savonnet, M.; Camarata, A.; Canivet, J.; Bazer-Bachi, D.; Bats, N.; Lecocq, V.; Pinel, C.; Farrusseng, D. Tailoring Metal–Organic Framework Catalysts by Click Chemistry. *Dalton Trans.* **2012**, *41*, 3945–3948. [CrossRef] [PubMed]
64. Cirujano, F.G.G.; Corma, A.; Llabrés i Xamena, F.X. Zirconium-Containing Metal Organic Frameworks as Solid Acid Catalysts for the Esterification of Free Fatty Acids: Synthesis of Biodiesel and Other Compounds of Interest. *Catal. Today* **2015**, *257*, 213–220. [CrossRef]
65. Mota, C.J.A.; Da Silva, C.X.A.; Rosenbach, N.; Costa, J.; Da Silva, F. Glycerin Derivatives as Fuel Additives: The Addition of Glycerol/Acetone Ketal (Solketal) in Gasolines. *Energy Fuels* **2010**, *24*, 2733–2736. [CrossRef]
66. Silva, P.H.R.; Gonçalves, V.L.C.; Mota, C.J.A. Glycerol Acetals as Anti-Freezing Additives for Biodiesel. *Bioresour. Technol.* **2010**, *101*, 6225–6229. [CrossRef]
67. Fatimah, I.; Sahroni, I.; Fadillah, G.; Musawwa, M.M. Glycerol to Solketal for Fuel Additive: Recent. *Energies* **2019**, *12*, 2872. [CrossRef]
68. Climent, M.J.; Corma, A.; Velty, A. Synthesis of Hyacinth, Vanilla, and Blossom Orange Fragrances: The Benefit of Using Zeolites and Delaminated Zeolites as Catalysts. *Appl. Catal. A Gen.* **2004**, *263*, 155–161. [CrossRef]
69. Sari, P.; Razzak, M.; Tucker, I.G. Isotropic Systems of Medium-Chain Mono- and Diglycerides for Solubilization of Lipophilic and Hydrophilic Drugs. *Pharm. Dev. Technol.* **2004**, *9*, 97–106. [CrossRef]
70. Piasecki, A.; Sokołowski, A.; Burczyk, B.; Kotlewska, U. Synthesis and Surface Properties of Chemodegradable Anionic Surfactants: Sodium (2-n-Alkyl-1,3-Dioxan-5-Yl)Sulfates. *JAOCS J. Am. Oil Chem. Soc.* **1997**, *74*, 33–37. [CrossRef]

71. Rapeyko, A.; Díaz Infante, J.C.; Llabrés i Xamena, F.X. Zr-Containing UiO-66 Metal–Organic Frameworks as Efficient Heterogeneous Catalysts for Glycerol Valorization: Synthesis of Hyacinth and Other Glyceryl Acetal Fragrances. *Mol. Syst. Des. Eng.* **2023**, *8*, 775–785. [CrossRef]
72. Otsuka, S.; Tani, K.; Yamagata, T.; Akutagawa, S.; Kumobayashi, H.; Yagi, M. Process for the Preparation of Enamines or Imines. EP Patent 68506, 3 January 1985.
73. Alaerts, L.; Seguin, E.; Poelman, H.; Thibault-Starzyk, F.; Jacobs, P.A.; De Vos, D.E. Probing the Lewis Acidity and Catalytic Activity of the Metal-Organic Framework $Cu_3(Btc)_2$ (BTC = Benzene-1,3,5-Tricarboxylate). *Chem.-A Eur. J.* **2006**, *12*, 7353–7363. [CrossRef]
74. Cirujano, F.G.; Llabrés Xamena, F.X.; Corma, A. MOFs as Multifunctional Catalysts: One-Pot Synthesis of Menthol from Citronellal over a Bifunctional MIL-101 Catalyst. *Dalton Trans.* **2012**, *41*, 4249–4254. [CrossRef] [PubMed]
75. Vandichel, M.; Vermoortele, F.; Cottenie, S.; de Vos, D.E.; Waroquier, M.; Van Speybroeck, V. Insight in the Activity and Diastereoselectivity of Various Lewis Acid Catalysts for the Citronellal Cyclization. *J. Catal.* **2013**, *305*, 118–129. [CrossRef]
76. Vermoortele, F.; Bueken, B.; Le Bars, G.; Van de Voorde, B.; Vandichel, M.; Houthoofd, K.; Vimont, A.; Daturi, M.; Waroquier, M.; Van Speybroeck, V.; et al. Synthesis Modulation as a Tool To Increase the Catalytic Activity of Metal-Organic Frameworks: The Unique Case of UiO-66(Zr). *J. Am. Chem. Soc.* **2013**, *135*, 11465–11468. [CrossRef] [PubMed]
77. Meerwein, H.; Schmidt, R. Ein Neues Verfahren Zur Reduktion von Aldehyden Und Ketonen. *Justus Liebigs Ann. Chem.* **1925**, *444*, 221–238. [CrossRef]
78. Ponndorf, W. Der Reversible Austausch Der Oxydationsstufen Zwischen Aldehyden Oder Ketonen Einerseits Und Primären Oder Sekundären Alkoholen Anderseits. *Angew. Chem.* **1926**, *39*, 138. [CrossRef]
79. Verley, A. Exchange of Functional Groups between Two Molecules. Exchange of Alcohol and Aldehyde Groups. *Bull. Soc. Chim. Fr* **1925**, *37*, 537.
80. Mautschke, H.H.; Llabrés i Xamena, F.X. MOF-808 as a Highly Active Catalyst for the Diastereoselective Reduction of Substituted Cyclohexanones. *Molecules* **2022**, *27*, 6315. [CrossRef]
81. Mautschke, H.H.; Llabrés i Xamena, F.X. One-Step Chemo-, Regio- and Stereoselective Reduction of Ketosteroids to Hydroxysteroids over Zr-Containing MOF-808 Metal-Organic Frameworks. *Chem.-A Eur. J.* **2021**, *27*, 10766–10775. [CrossRef]
82. Dodge, J.A.; Lugar III, C.W. Alcohol Inversion of 17b-Steroids. *Bioorg. Med. Chem. Lett.* **1996**, *6*, 1–2. [CrossRef]
83. Han, G.-D.; Lin, Z.-Y.; Yan, C.-P. Synthesis of Musk Androgen 5a-Androstane-3b,17a-Diol. *Zhongguo Yiyao Gongye Zazhi* **1994**, *25*, 490–491.
84. Ohta, T.; Zhang, H.; Torihara, Y.; Hida, T.; Furukawa, I. Practical Synthesis of Androgen: The Efficient Transformation of 17-Oxo Group to 17a-Hydroxy Group. *Steroids* **1998**, *63*, 630–632. [CrossRef] [PubMed]
85. Göndös, G.; Orr, J.C. Reduction of Steroid 17-Ketones by Enantiomeric Chiral Reducing Agents. *J. Chem. Soc. Chem. Commun.* **1982**, 1238–1239. [CrossRef]
86. Wang, A.; Zhou, Y.; Wang, Z.; Chen, M.; Sun, L.; Liu, X. Titanium Incorporated with UiO-66(Zr)-Type Metal–Organic Framework (MOF) for Photocatalytic Application. *RSC Adv.* **2016**, *6*, 3671–3679. [CrossRef]
87. Bakuru, V.R.; Churipard, S.R.; Maradur, S.P.; Kalidindi, S.B. Exploring the Brønsted Acidity of UiO-66 (Zr, Ce, Hf) Metal-Organic Frameworks for Efficient Solketal Synthesis from Glycerol Acetalization. *Dalton Trans.* **2019**, *48*, 843–847. [CrossRef]

Disclaimer/Publisher's Note: The statements, opinions and data contained in all publications are solely those of the individual author(s) and contributor(s) and not of MDPI and/or the editor(s). MDPI and/or the editor(s) disclaim responsibility for any injury to people or property resulting from any ideas, methods, instructions or products referred to in the content.